# Synthesis of nanoporous materials for preconcentration and determination of trace elements by ICP-AES
# Investigation and elimination of the memory effects of mercury, gold, silver and boron in ICP-AES

by

Wencan Chen

A thesis
Presented to the Department of Chemistry
in partial fulfillment of the requirements
for the degree of
Master of Science

December 1999
Brock University
St. Catharines, Ontario

# Abstract

Nanoporous materials with large surface area and well-ordered pore structure have been synthesized. Thiol groups were grafted on the materials' surface to make heavy metal ion pre-concentration media. The adsorption properties of the materials were explored. Mercury, gold and silver can be strongly adsorbed by these materials, even in the presence of alkaline earth metal ion. Though the materials can adsorb other heavy metal ions such as lead and copper, they show differential adsorption ability when several ions are present in solution. The adsorption sequence is: mercury > = silver > copper >> lead and cadmium.

In the second part of this work, the memory effects of mercury, gold, silver and boron were investigated. The addition of 2% L-cysteine and 1% thiourea eliminates the problems of the three metal ions completely. The wash-out time for mercury dropped from more than 20 minutes to 18 seconds, and the wash-out time for gold decreased from more than 30 minutes to 49 seconds. The memory effect of boron can be reduced by the use of mannitol.

## Acknowledgements

I would like to express my sincere thanks to my supervisor, Professor Ian D. Brindle, for his encouragement, advice, patience and support throughout this thesis. Thank you also to the members of my committee, Dr. Fred Capretta and Dr. Jack Miller, for their time and invaluable suggestions.

Special thanks to our group members: Sirirat (Jing) Chanvaivit, Sarah Overduin, Renjin Wang, Chris Robertson, Amy Jones, Brett Wales and all Chinese friends: Huangshu (John) Lei, Jinhui (Scott) Deng, Rowei Mo, Ye Feng, Dr. Jianxin Gu and Dr. Quan Zhuang.

I would also thank all staff, faculty members and friends in the Department of Chemistry.

Thanks to my husband Dong Liu, for his patience and generous support when I needed it most. Most of all, I would like to thank my parents and sisters, for their endless trust, love, encouragement and support. They make me strong.

# Table of Contents

# List of Figures

# List of Tables

# Synthesis of nanoporous materials for preconcentration and determination of trace elements by ICP-AES Investigation and elimination of the memory effects of mercury, gold, silver, and boron in ICP-AES

## 1. Introduction

### 1.1 Inductively coupled plasma atomic emission spectroscopy (ICP-AES)

Atomic emission spectroscopy has been long used as a standard method for the determination of elements. The development of the inductively coupled plasma (ICP) as an atomic emission source made this method even more popular. The advantages of ICP include: simultaneous multi-element determination capability, fast sample throughput, high level of accuracy and precision, low detection limits, wide linear calibration range (over five orders of magnitude of concentration), relatively low sample consumption.

The principles of ICP-AES are explained in many books.[1,2] In an inductively coupled plasma source, an induction coil is set around a quartz tube. Alternating current flows through this coil at a frequency of around 27.1 MHz or 40 MHz. While argon gas passes through the quartz tube, it is ionized by the radio-frequency magnetic field provided by the coil. The fast-moving and colliding cations and electrons produce intense thermal energy. A flame-shaped plasma forms near the top of the torch. Temperatures in the plasma range from 6000 to 10,000 K. A sample aerosol is generated

by a nebulizer and passes through the spray chamber, then enters the plasma. The sample is dried, atomized, excited or ionized in this plasma. Then the emissions of photons of the analytes enter the spectrometer slit. The emission spectra of the elements are separated and their intensities are measured. This stable and high temperature excitation source ensures the analytical precision and the detection capability for a wide range of elements.

Other widely used methods in trace element determination include atomic absorption spectrometry (AAS) and ICP mass spectrometry. The AAS method can usually determine only one element at one time and its calibration linear range is not as broad as the ICP-AES method. ICP-MS has the lowest detection limit among the three methods, but it is much more expensive than the other two. In this work, we developed techniques that can lower detection limits and improve precision of ICP-AES. Our work is in two parts: one involves the synthesis of nanoporous materials for preconcentration and determination of trace elements by ICP-AES. The other is the development of techniques for the elimination of memory effects from some problematic ions in their determination by ICP-AES.

## 1.2 Preconcentration

### 1.2.1 Preconcentration in ICP-AES

The use of a preconcentration step is one of the more effective ways of increasing sensitivity, lowering detection limit and widening the scope of determination techniques. This operation can be conveniently performed by using a mini-column packed with a suitable adsorbent or ion-exchange material, or by using liquid-liquid extraction.[3] Many

supports have been used for the chelating groups, such as styrene-divinylbenzene copolymers,[4,5] cellulose, silica gel, sepharose and controlled-pore glass. Different chelating compounds, such as 8-hydroxyquinoline,[6] mercapto derivatives,[7] oxine compounds,[8] hydroxybenzoyl derivatives[9] and amine[10] compounds, are immobilized on the surface of the support.

During the past ten years, the most frequently used chelating compounds have been complexing reagent containing amine, thio carbamates, carboxylate or/and hydroxyl groups. In early work in 1986, ethylenediaminetriacetate groups were bonded to silica gel. Water samples containing trace elements were buffered at pH 5 and then passed through this grafted silica gel.[11] In 1988, hexamethylenedithiocarbamate was grafted to cellulose (Cell-HMDC).[12] Trace heavy metal ions were collected using a batch-procedure. Compared to reversed-phase-sorbents, Cell-HMDC was better since it was independent of salt content (e.g., 30g/L NaCl). But other complexing substance, like EDTA or CN-, could decrease its recovery. 1-(2-pyridyl azo)-2-naphthol-polyurethane foam was also studied for preconcentration of metal ions.[13]

Conformationary flexible amino-carboxylic groups were introduced into sorption filters as well as column material using in flow injection ICP-AES.[14,15] Minicolumns packed with fibers and chelating sorbents with amine, 8-hydroxyquinoline and 3(5)-methylpyrazole groups were used for the preconcentration of Cu and Au.[16] Polyamine chelating ion resins[17] and activated carbon fibers[18] were also used in preconcentration studies of heavy metal ions. Also, amidoxime chelating groups were covalently bound to the surface of a textile encased in a common 35 mm slide holder. The device was put in

river water to collect metal ions. Semiquantitative analysis of trace metal ions was achieved by this technique.[19]

In the above methods, the elements collected are mostly limited to Pb, Cu, Zn, Cd, Mn, Fe. One of the most important environmental toxic elements, Hg, is not reported enough. Also, from the property of those amino containing complexing reagents, we can see that the adsorption of the ions is largely influenced by the pH of the solution.

In recent years, new research has attempted to optimize the loading effectiveness of preconcentration media, not only in view of the total capacity with respect to the ligand, but also taking into account that only the adsorbing species, with chelating groups at the surface in a favourable steric position, will be able to fix the metal ions.[20,21]

There is a kind of new porous material that has aroused widespread interest of scientists. The characteristics of this kind of materials are their well-organized pore structure, narrow pore size distribution and large surface area. These features make them ideal support material for sample pre-concentration. In addition, thio containing organic group can be grafted onto this kind of inorganic support. This combination will naturally produce a material that has strong adsorption of thiophilic metals, which is an important property of heavy metal ions.

### 1.2.2 Nanoporous materials

#### 1.2.2.1 Basic chemistry: formation mechanism, applications

Nanoporous materials are grouped into three classes according to their pore diameters: d< 2nm, microporous; 2nm =< d <= 50nm, mesoporous; d> 50nm,

macroporous. Mesoporous materials have pore size similar to small biological molecules, macromolecules, metal clusters, and organometallic compounds. Thus mesoporous materials with good pore accessibility and narrow pore size distributions (not all the mesoporous materials have narrow pore size distribution) may be useful as hosts, supports, catalysts, or separation media for these species. Since most of the ions' radii are less than 0.15nm, even less than 0.1, after coordinated with $H_2O$, their total radii should be less than 0.5nm. For our application, a material with a pore size between mesoporous and microporous is already big enough to let heavy metal ions to get into the channel and attach to the function groups on the surface.

The synthesis of ordered mesoporous material was first reported by researchers of Mobil Oil in 1992[22,23]. Compared to amorphous silica, this kind of mesoporous silica has very high surface area, ordered pore structure (mostly hexagonal packed arrays of channels) and narrow pore size distribution. From 1992, this kind of material research has become a very active area because mesoporous silica has a wide range of controllable physical-chemical properties such as pore size, surface hydrophilicity and elemental composition. So they have found many applications in catalysis. Different kinds of mesoporous materials have been prepared, including alumina, zirconia, titania, niobia, tantalum oxide and manganese oxide. In most cases, the pore structure of non-silica-based materials is not as well-organized as silica-based materials. Scientists gradually realized that the high surface area, pore size selectivity, mechanical stability, as well as reduced swelling of the material, offer many potential sorption separation applications. So it is quite reasonable to introduce this material to the application area of preconcentration in ICP-AES.

Well-defined mesoporous material can be synthesized by templating molecular metal oxide precursors around surfactant assemblies. Four reagents are needed: small metal-oxide ions, surfactant, solvent, and chemicals to adjust the pH. In the synthesis, the material is prepared in the following way: a ceramic precursor (tetramethoxysilane, TMOS, in our experiment) is mixed with a basic aqueous solution of a micelle-forming cationic surfactant (cetyltrimethylammonium bromide, CTAB, in our work). The TMOS is hydrolyzed to form small anionic oligomers that can coordinate with the surfactant headgroups. The strong interaction between the silica species and the surfactants leads to phase separation of the silica/surfactant arrays into microdomains that have an ordered liquid crystalline structure. The surfactants can be removed from the inorganic framework by solvent extraction or calcination. Study shows that the structure and the pore size of the material largely depend on the aggregation process of the surfactant. The tendency of the hydrocarbon part of the surfactant to associate with itself is a primary driving force in surfactant aggregation. Therefore, the lipophilic chain length and head group substituents are important structure factors. However, the inorganic anion partner of the cationic surfactant also helps to mediate this organization process. Also, the ceramic precursor anion participates in the organization process of surfactants, leading to ordered liquid crystal like structures. The extent to which the silicate anion influences the surfactant organization depends on the silicate-surfactant affinity relative to halide-surfactant or hydroxide-surfactant affinity. Different structures can be formed by varying the ceramic precursor concentration while maintaining constant surfactant concentration. The whole procedure is illustrated in Figure 1.[24]

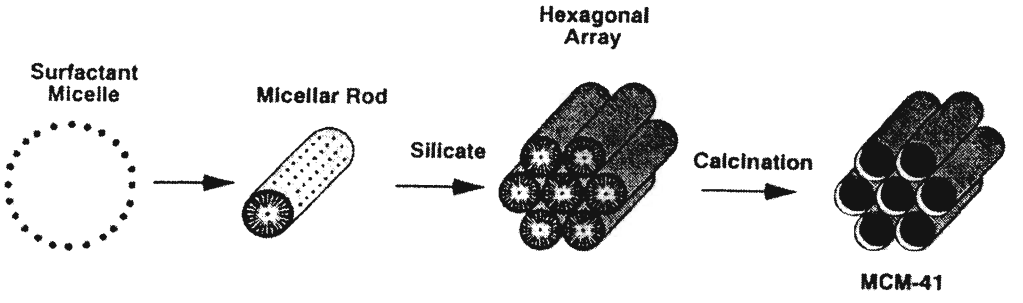


Figure 1. Formation pathway of ordered mesoporous silicates
(modified from reference 24)

In our work, we also adopted a neutral templating synthesis route. The formation of the mesostructure happens through the aggregation of neutral primary amine surfactant molecules (dodecyl amine, in our work) into neutral rod-like micelles. The inorganic precursor (say, tetraethoxysilane, TEOS, in our work) hydrolyzed into neutral intermediate species $Si(OC_2H_5)_{4-X}(OH)_X$. And these species attached themselves to the lone electron pairs on the surfactant head groups by H-bonding interactions. In this surfactant-inorganic complex, the surfactant part can be viewed as a hydrophobic tail and the inorganic precursor as a big head group. Then these complexes form rod-like micelles. Further hydrolysis and condensation of the silanol groups on the micelle-solution interface produce short-range hexagonal packing of the micelles and framework wall. This procedure is illustrated in Figure 2.[25]

Functional organic group can be brought further into the inorganic framework, thereby modifying it for specific applications. In our work, thio groups were introduced into the ordered inorganic support in order to make a heavy metal ion absorbent. There are two ways to put functional groups to the support: one is grafting other molecules (such as siloxanes) to the surface hydroxyl groups of the inorganic material, the other is incorporating functionalities directly in the synthesis. Each way has its pros and cons. In the postsynthesis grafting method, it is easier to get well-defined porous supports. But the surface concentration of organic group is limited by the number of reactive surface silanol groups present and by diffusion limitations. In direct incorporation synthesis, it is harder to obtain a well-ordered structure than in the first method. While it is obvious that the second way is much simpler, in this work we tried both methods.

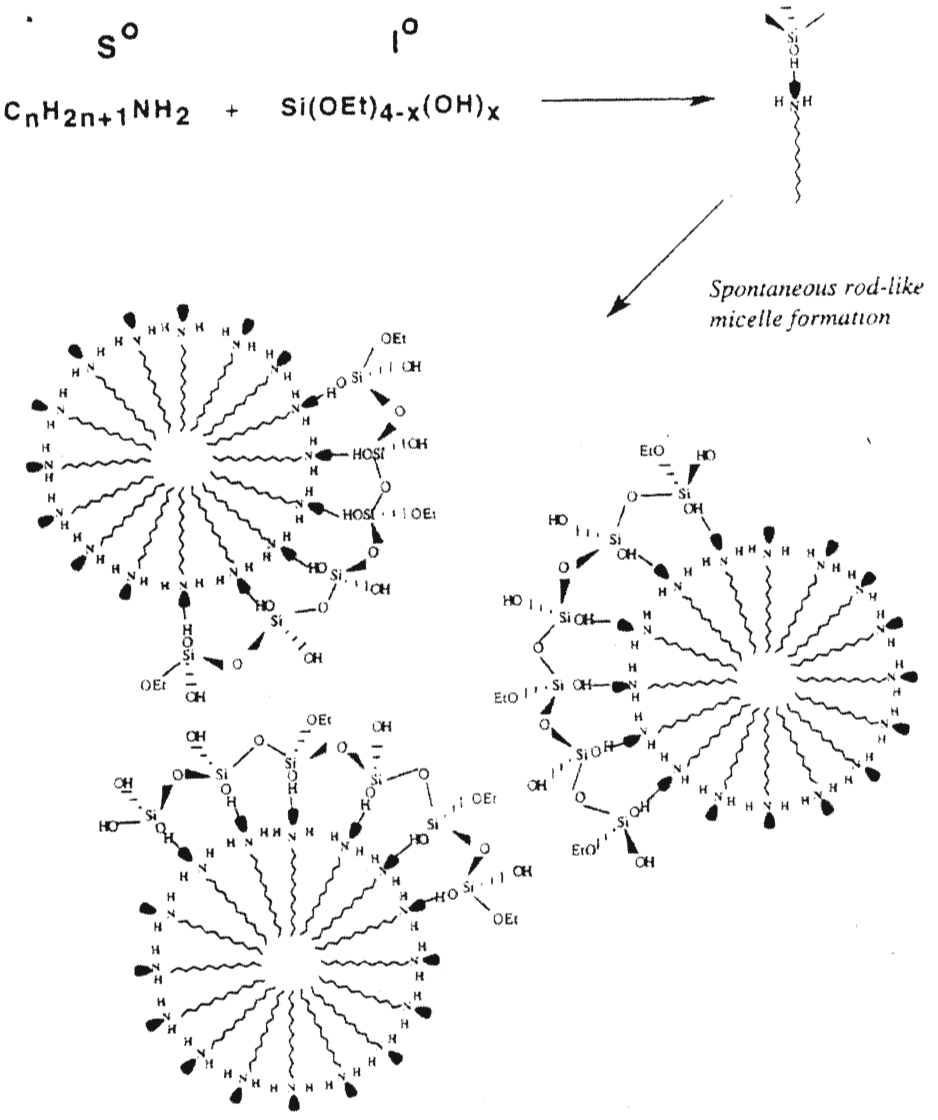


Figure 2. A neutral templating mechanism to mesoporous material

### 1.2.2.2 Characterization techniques: NMR, Nitrogen adsorption analysis

#### 1.2.2.2.1 Solid State NMR

Solid State NMR is a very useful tool for characterizing the structure for support material. In our work, magic angle spin $^{29}Si$ NMR was used. For amorphous silicates, the $^{29}Si$ NMR are broad peaks in the range of –70 to –120 ppm with respect to TMS. For crystalline silicates, the peaks are much sharper. Different types of Si species are represented by $Q^n$ notation. Their notations and chemical shifts are given in Figure 3[26] $Q^0$ denotes the monomeric orthosilicate anion $SiO_4^{4-}$, the Si atom is not connected to other Si atoms. $Q^1$ refers to the end-groups of chains. It means a Si atom is connected to one Si atom by an O atom. $Q^2$ means a Si atom is connected to two other Si atoms by two O atoms, so it is middle groups in chains or cycles. Similarly, $Q^3$ refers to branching groups and $Q^4$ means cross-linked groups. In situations where the Si atom is directly connected to one carbon atom (e.g. to an alkyl chain), a $T^n$ terminology is now used to describe the condensation products of RSi(OR).[27] We will use this notation to describe our grafted mercaptopropylsilane groups. The notations are given in Figure 4. The notation range is from $T^0$ to $T^3$. Since, among the four bonds around Si, one is with C, not O, one Si atom can connect to a maximum of three other Si atoms via O atoms.

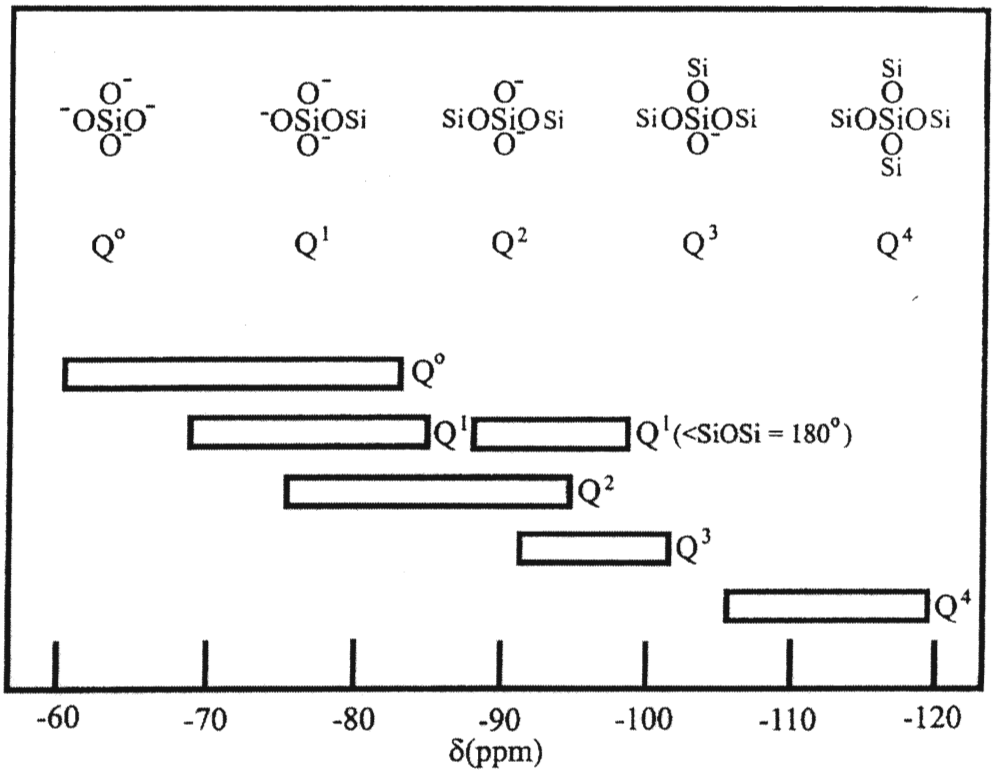


Figure 3. Ranges of $^{29}Si$ chemical shifts of $Q^n$ units in solid silicates

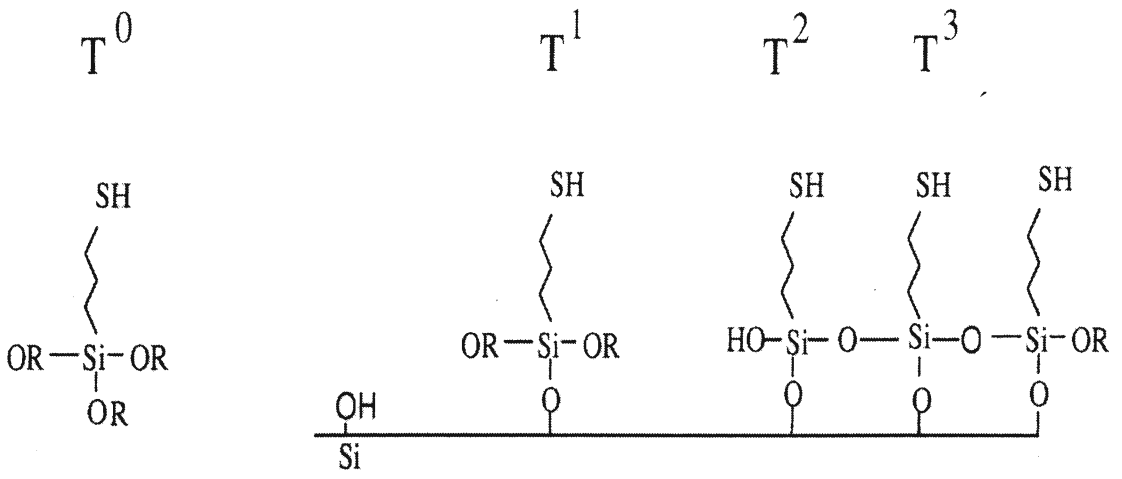


Figure 4. $T^n$ notations

1.2.2.2.2 Nitrogen adsorption-desorption analysis

Nitrogen adsorption-desorption analysis is a widely used method for total surface area and pore size measurements. In this physical characterization process, $N_2$ molecules are physically adsorbed on sample surfaces. The quantity of gas adsorbed and the pressure are recorded at a constant temperature. An isotherm is obtained from these data. Several calculation models can be applied to the data to obtain surface area and pore size distribution. The BET and BJH calculations were used in our analysis.

The BET (Brunauer, Emmett and Teller) method is the most commonly used calculation method for the characterization of surface area. It can be represented as:

$$P/[V_a(P_0-P)] = 1/V_mC + [(C-1)/V_mC] \times P/P_0$$

Where $V_a$ is the volume adsorbed at relative pressure $P/P_0$. $V_m$ is the volume of monolayer capacity. C is a constant related to the enthalpy of adsorption.

After determining $V_m$ from the above function, The BET surface area is then determined from the following expression:

$$S = (V_m \times N_a \times A_m)/M_v$$

Where S is the BET surface area, $N_a$ is Avogadro's constant. $A_m$ is 0.162 $nm^2$ here. $M_v$ is the gram molecular volume (22414 mL).

There are several ways to calculate pore size distribution. Here we used is BJH (Barrett, Joyner and Halenda) method. It is derived from the Kelvin equation:

$$RT \ln (P/P_0) = -2\gamma V_m/ R_k$$

Where $R_k$ is Kelvin radius, R is gas constant and T is the boiling point of nitrogen. $\gamma$ is the adsorbate surface tension at T and $V_m$ is the molar volume of nitrogen.

The thickness of the nitrogen film adsorbed on the walls of the pore at a given relative pressure is:

$$t = 3.54 \times [5/(2.303\log (P/P_0))]^{1/3}$$

The actual radius of the pore $R_p$ is:

$$R_p = R_k + t$$

## 1.3 Memory effect:

Another important part of our work was the investigation and elimination of the memory effect that presents significant challenges in the determination of some heavy metal ions.

The sample introduction system is the most important and the weakest part of an ICP-AES instrument[28]. Though the determinations of elements using ICP-AES is a well known, convenient and precise technique, the determination of mercury, gold and silver are seriously limited by their physical memory effect which has its origins in the sample introduction system. Nebulizers and spray chambers do not behave conservatively with all elements. So-called high field strength elements (HFSEs), such as Zr, Nb, Hf, Ta, Th, U, and other elements, including Sn, W, and Mo have been reported to exhibit significant memory effects. These effects have led to "spurious results" due to transfers between high concentration samples and calibration samples.[29] Similarly, gold, silver, mercury and boron have been reported to exhibit memory effects in a number of applications.[30,31,32,33] The dependency of detection limits on the memory effect was identified by Newman,[31] who noted that ICP-MS systems exhibit memory effects that have a physical origin. The

economics of the memory effects are significant for the analyst who is faced with the need to perform multi-element determinations with high throughput rates.

Memory effects manifest themselves in two ways and can be defined by the wash-in and wash-out times. The most obvious phenomenon is the wash-out time which, for "sticky" elements, may be as long as an hour. Varnes provided a reasonable criterion for wash-out time by suggesting that this is the time required for the analyte signal to drop to 0.1% of the steady state signal after the wash solution is introduced.[34] The second way that the memory effect can be observed is in the process of washing in. A plausible explanation of the memory effect is that physical chemical processes occur, such as adsorption, where active sites for retention of the analyte are occupied during the initial wash-in process and are slowly released during wash-out. Hence, during the initial introduction of the sample, the analyte in the sample is depleted until all active sites are in equilibrium with the solution. Dale and Buchanan[35] suggested that the attainment of 95% of the steady-state signal was a suitable criterion for wash-in time, but Varnes[34] disputed this criterion, preferring a 99% level as more reasonable, since the remaining 1% lies within the error envelope of the determination.

For the laboratory faced with samples containing wildly varying concentrations of analytes, and a need to measure close to the detection limits with some, the $3\sigma$ criterion (3 times the standard deviation of the blank) is a more prudent measure for defining the wash-out time. Thus, when analyte signals fall within $\pm 3\sigma$ of the baseline value, this might be a better measure of wash-out if a high concentration sample were to be followed by one of low concentration. For low concentrations of analyte, or for weaker signals, the 0.1% criterion may be more stringent than the $3\sigma$ one, thus leading to some confusion.

Several laboratories have proposed remedies for a number of the elements described above. Moreton and Delves used aqueous ammonia and diammonium EDTA to eliminate memory effects from low (ng $ml^{-1}$) concentrations in the determination of mercury by ICP-MS.[36] Hydrobromic acid has been used both at Atomic Energy Canada Limited (AECL)[37] and the National Institute for Standards and Technology (NIST)[38] to reduce memory effects from mercury. A number of reagents have been used to reduce memory effects from boron, including ammonia, NaF, Triton X-100 and mannitol.[32]

The goal of the first part of our work was to find a preconcentration material that can overcome some of the shortcomings of the previous materials as well as have high absorption capacity. Also, we wished to explore its potential applications. The second part of the work explores remedies for the memory effects of gold, mercury and silver and the results of our investigations into the memory effect of boron.

# 2. Experimental

In our work, functionized nanoporous materials were synthesized, they were characterized by solid-state $^{29}Si$ nuclear magnetic resonance and nitrogen adsorption desorption analysis. Their heavy metal ion adsorption features were tested by ICP-AES. The memory effect research was all carried out using ICP-AES.

## 2.1 Synthesis of nanoporous materials

### 2.1.1 Sequential method[39,40] (Method I)

Tetraethyl orthosilicate 0.2 mol (41.7g) was added under vigorous stirring to a solution of dodecyl amine (0.054 mol, 10.0g) in ethanol (1.818mol, 83.6g) and deionized

water (5.92 mol, 106.6g). Then the mixture was aged at ambient temperature for 18 hours. The resulting hexagonal mesoporous material was air-dried on a glass plate. Then the template was removed by refluxing the material with 360mL ethanol for 24 hours. After filtering off, the material was refluxed with another portion of 360mL ethanol for 18 hours, then filtered off, vacuum dried at 120°C and 15 mm Hg, overnight, 13.43g of material was obtained. The material was refluxed with 13.4g 3-mercaptopropyltrimethoxysilane in 300 mL dry toluene for 48 hours. The functionalized product was filtered, washed several times with toluene followed by ethanol. In order to remove the residual organosilane, the material was divided into two portions, both were subjected to Soxhlet extraction over ethanol (600 mL), one portion for 48 hours, the second portion for 72 hours. At last the material was filtered, vacuum dried at 75°C and 0.5 mm Hg, for 6 hours.

### 2.1.2 Homogeneous method[41] (Method II)

Cetyltrimethylammonium bromide (CTAB) 8.76g was dissolved in 280 mL $H_2O$ with 2.20g NaOH. (3-Mercaptopropyl)triethoxysilane (MPTS) 11.8g was mixed with 22.16g tetramethoxysilane (TMOS). Then the MPTS and TMOS mixture was added to the surfactant containing solution with stirring. The whole solution was stirring at room temperature for 12 hours, followed by heating at 95°C for 36 hours. To remove the surfactant, the material was refluxed with a mixture of 12g HCl and 288g MeOH for 24 hours. This extraction was repeated 3 times. Then the material was filtered, washed with $CH_2Cl_2$, and vacuum dried at 75°C and 15mm Hg for 24 hours.

## 2.2 Loading capacity tests

Loading capacities of mesoporous material, prepared by Method I, were tested. The experiments were performed in the following way: 100 mL each of $Hg^{2+}$ solutions (0 to 100μg $ml^{-1}$) were prepared at pH 5. Each solution was divided into two portions of 50 mL. 10 mg of material, prepared by method I, was suspended in 50 mL of the solution to equilibrate at room temperature. The other 50 mL solution was used as "adsorption blank". After 18 hours the material was filtered off. The $Hg^{2+}$ uptake was measured by comparing the $Hg^{2+}$ concentration difference in the two portions of the solutions. The loading capacity of $Ag^{+}$ was tested in a similar way, except that the pH of the solutions were 3.5.

## 2.3 Column adsorption and desorption study

In the column adsorption and desorption experiment, Waters Sep-Pak cartridges were used, the inside packing materials were dumped out, leaving the septum at one end, then 10 mg portion of our material was loaded into the cartridge. At the end of the column, tygon tubing was connected to a peristaltic pump. Solutions were then passed through this device.

## 2.4 Memory effect study

In our memory effect study, we applied the following experiment procedure to obtain our results: To obtain washout curves, a blank solution containing the appropriate complexing agent and 1% (v/v) nitric acid, was aspirated into the plasma followed by a solution containing the analyte and complexing agent. After sufficient time had been

allowed for a steady signal to be established, the blank solution was reintroduced into the system.

## 2.5 Instrumental

### 2.5.1 NMR

The synthesized samples were analyzed on a Bruker DPX300 multinuclear Fourier transform NMR with a standard bore Bruker 4 mm high speed MAS probe. Samples were packed into 4mm zirconia rotors. The $^{29}Si$ spectra were obtained at 59.62 MHz using cross polarization with proton decoupling during acquisition. Spectra were referenced to tetramethylsilane ( $\delta$ = 0 ppm). Samples were spun at 4 kHz with a 5 ms cross-polarization contact time and a 5 s delay between pulses. The spectral window is 18 kHz with approximately 4,000 FID's collected.

### 2.5.2 Nitrogen adsorption-desorption analysis

The samples were tested on a Coulter SA3100 surface area analyzer. About 0.1 g of sample was outgassed at 200°C for 1 hour under high vacuum to remove anything physisorbed onto the surface. Surface areas were determined by BET adsorption method and pore volumes by BJH method on the desorption branch of the isotherm at 77K, using $N_2$ as the adsorbate.

### 2.5.3 ICP-AES operation parameters

A commercial ICP-Emission Spectroscopy system (Optima 3300DV, Perkin Elmer, Norwalk, CT) was used for all the experiments in testing the heavy metal ions in solution in our pre-concentration work and also the elimination of memory effect work.

The experimental operating parameters are listed in Table 1. Parameters A were used in pre-concentration work. Parameters B and C were used in memory effect elimination work. Except where indicated, conditions listed under parameters B were used for all memory effect elimination work.

Table 1. Operating conditions for ICP-AES analysis

| | Parameters A | Parameters B | Parameters C |
|---|---|---|---|
| RF power (kW) | 1.3 | 1.3 | 1.3 |
| Frequency (MHz) | 40 | 40 | 40 |
| ICP torch | Quartz | quartz | Quartz |
| Torch Injector | Alumina | alumina | Ceramic alumina |
| Injector i.d. (mm) | 2.0 | 2.0 | 2.0 |
| Nebulizer Flow (L/min) | 0.85 | 0.85 | 0.85 |
| Auxillary Flow (L/min) | 0.5 | 0.5 | 0.5 |
| Plasma Flow (L/min) | 15 | 15 | 15 |
| Nebulizer | Gem cone | Gem cone | Cross-Flow |
| Spray chamber | Glass Cyclonic | Glass Cyclonic | Scott-type double pass |
| Sample pump rate (ml/min) | 1.0 | 1.0 | 1.0 |
| Read time (second) | Automatic | 6 | 6 |

## 2.6 Reagents and chemicals

### 2.6.1 Chemicals used in synthesis

Cetyltrimethylammonium bromide: Aldrich

Dodecyl amine: Aldrich, 98%

Ethanol: Fluka, analytical grade

Tetraethoxysilane (TEOS): Aldrich, 98%

Tetramethoxysilane (TMOS): Aldrich, 98%

(3-mercaptopropyl) triethoxysilane: Fluka, Techn. > 80% GC

(3-mercaptopropyl) trimethoxysilane: Aldrich, 95%

### 2.6.2 Chemicals used in all ICP-AES tests

ICP standards of mercury were obtained from PerkinElmer company, silver, gold, lead, copper, cadmium, calcium, ruthenium and boron were from SCP science. All the solutions were diluted with deionized water. High purity nitric acid (Caledon) and hydrochloric acid (EM Science) were used. The ammonia (Caledon) and hydrobromic acid (Fisher Scientific) were of analytical grade. L-cysteine (SIGMA), thiourea (Aldrich, Inc.) and mannitol (Eastman Organic Chemicals) were used in the preparation of various standard solutions.

# 3. Results and discussion for pre-concentration study

## 3.1 NMR results

The solid-state $^{29}Si$ NMR for material prepared from Method I are shown in Figure 5 and 6. Figure 5 is the material without grafting of the functional group. Figure 6 is the material with the functional group. In Figure 5, the peak at –108.8 ppm is assigned to $Q^4$ species and the shoulder peak comes from the $Q^3$ species. In the grafted material (Figure 6), the –110.7 ppm peak is from $Q^4$ species and the decrease of the shoulder indicates a decrease of the $Q^3$ species, which are the surface Si-OH groups. Also, there is a small peak at –50 ppm is assigned to the $T^1$ species from the grafted mercaptopropylsilane moieties.

Figure 7 shows the solid-state $^{29}Si$ NMR result for material prepared from Method II. The peaks at –102 ppm and –111 ppm are assigned to $Q^3$ and $Q^4$ species. The peak at –67 ppm is assigned to $T^3$ silicon atoms from the grafted groups, and the shoulder at approximately –55 ppm is from the $T^2$ species.

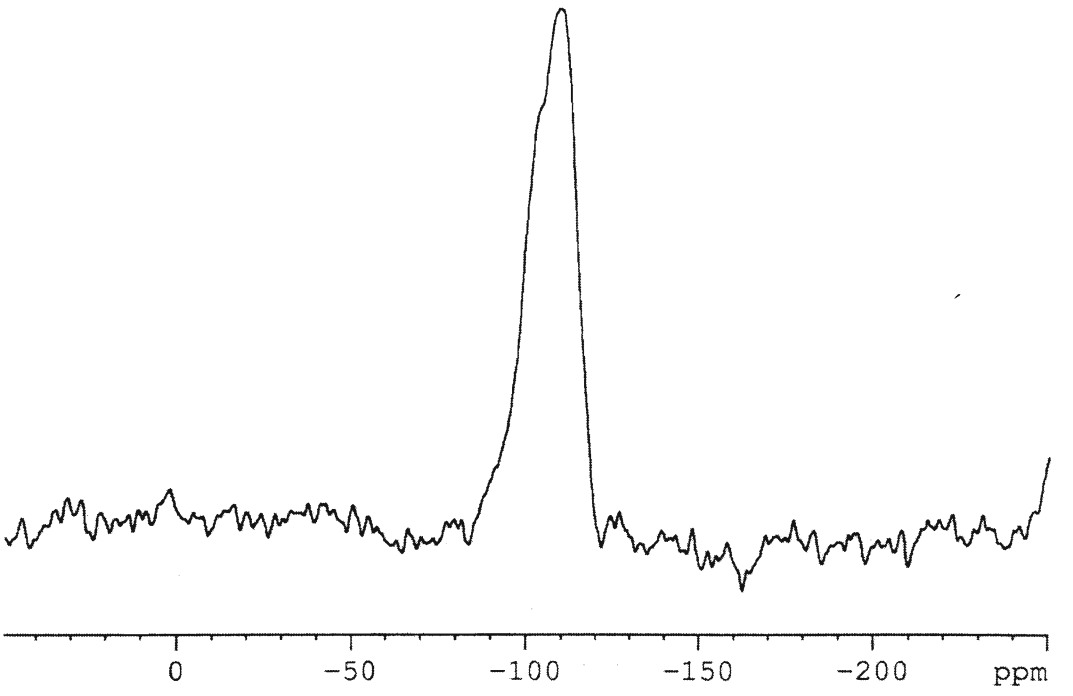


Figure 5. $^{29}$Si NMR for Material I
(only support, without functional group)

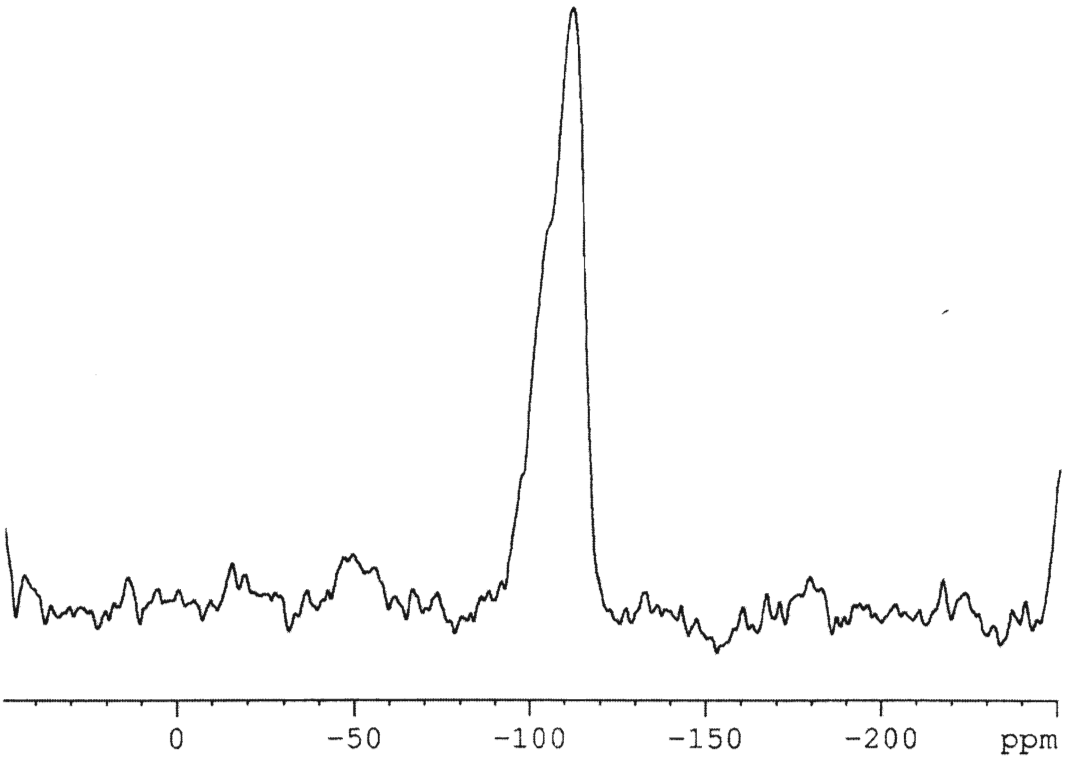


Figure 6. $^{29}$Si NMR for Material I (with functional group)

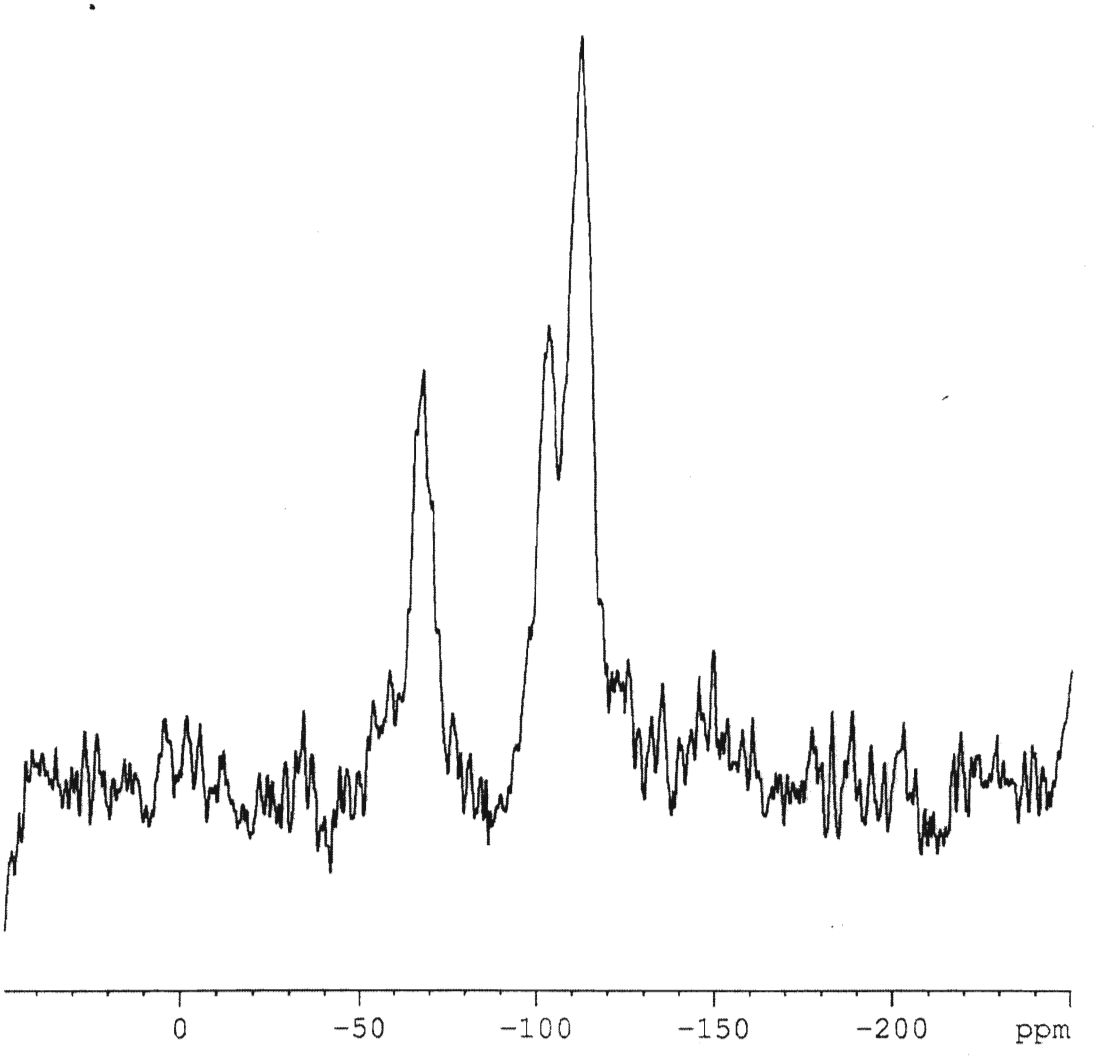


Figure 7. $^{29}$Si NMR for Material II

## 3.2 Nitrogen adsorption-desorption results

The surface area for the material prepared by Method II was found to be 1109.37 $m^2/g$. And the total pore volume is 0.5977 $cm^3/g$. These values are larger than those in the reference paper[39] (792 $m^2/g$, 0.47 $cm^3/g$). Figure 8 shows the adsorption-desorption isotherm. The shape of the isotherm indicates that the material falls into the range between zeolites and mesoporous material (Figure 9[25]). The instrument does not provide results for pore size less than 6nm, but in the reference paper, the reported size is 1.4 nm.

For the material prepared by Method I, the surface areas were determined for both the support material and the functionized material. The surface area for the support material was 1224.5 $m^2/g$ and decreased to 1105.1 $m^2/g$ for grafted material. The pore volume decreased from 0.85 $cm^3/g$ to 0.62 $cm^3/g$. This observation is consistent with the presence of grafted species attached to the framwork walls of the material. The shapes of the isotherm shown in Figure 10a and 10b agree well with reports for mesoporous material. The pore sizes reported in the reference paper are 3.6 nm and 2.7 nm, for the support and grafted material, respectively.

Surface Area Report

| | |
|---|---|
| BET Surface area | 1109.37 sq.m/g |
| Correlation Coefficient | 0.99839 |

Total Pore Volume Report

| | |
|---|---|
| Total Pore Volume | 0.5977 cc/g |
| (Ps/Po = 0.9814, Adsorption) | |

Desorption BJH Pore Size Distribution

| Pore Dia. Range(nm) | Pore Volume (cc/g) | % |
|---|---|---|
| Under 6 | 0.03066 | 36.28 |
| 6 - 8 | 0.00563 | 6.66 |
| 8 - 10 | 0.00335 | 3.96 |
| 10 - 12 | 0.00261 | 3.09 |
| 12 - 16 | 0.00280 | 3.32 |
| 16 - 20 | 0.00232 | 2.75 |
| 20 - 80 | 0.01775 | 21.01 |
| Over 80 | 0.01938 | 22.93 |

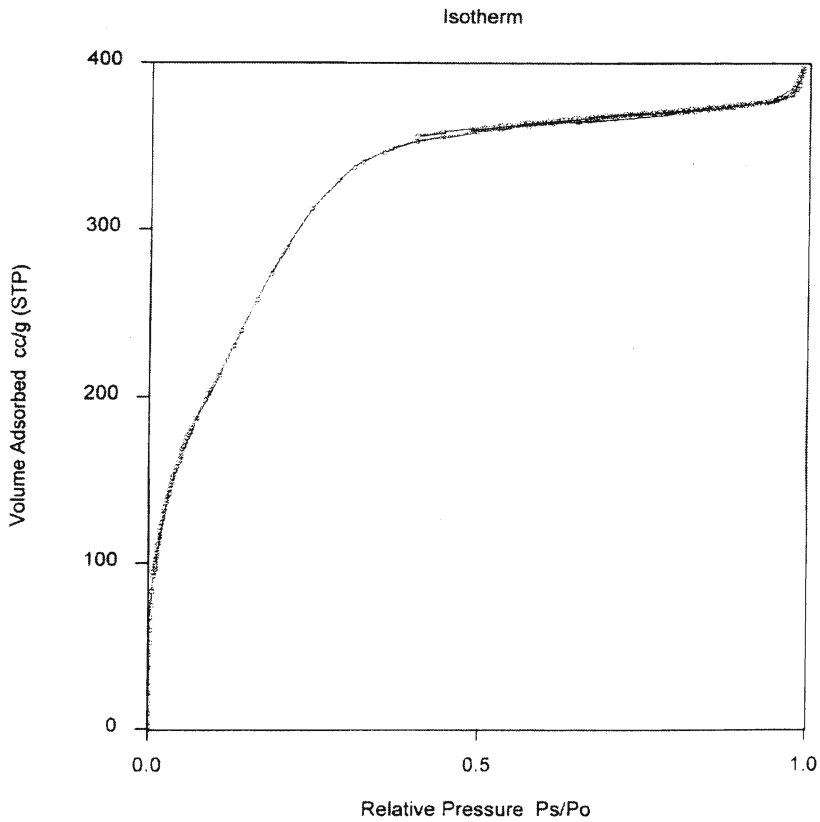


Figure 8. Nitrogen adsorption-desorption result for Material II

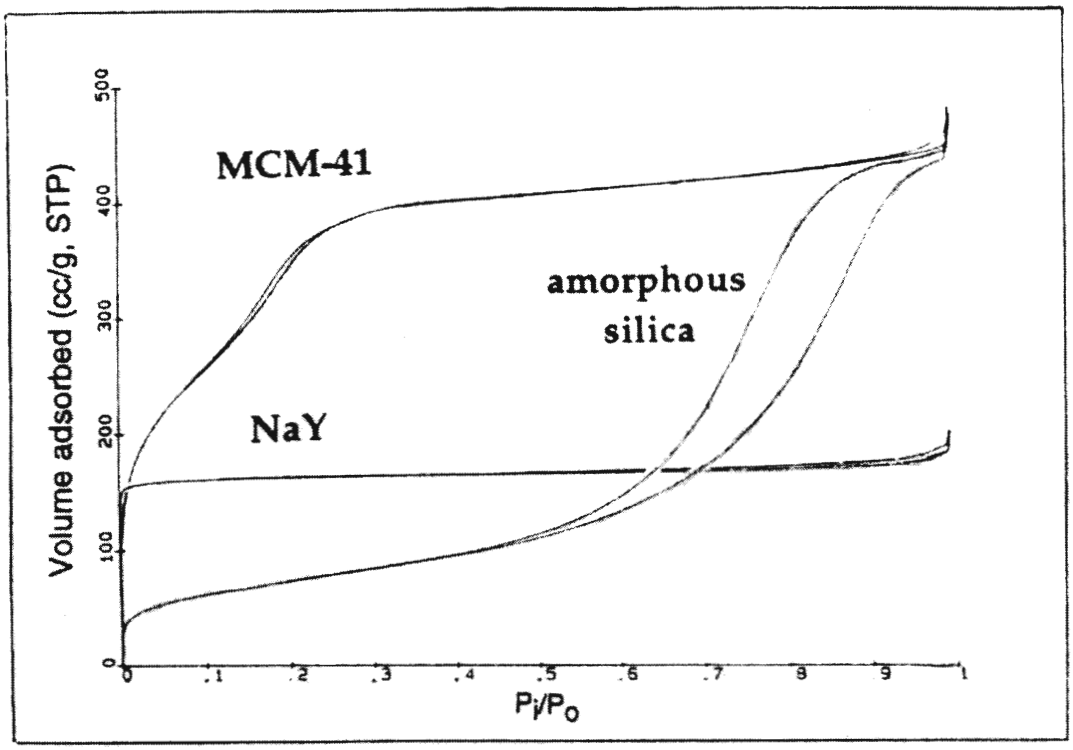


Figure 9. $N_2$ adsorption-desorption isotherms for amorphous silica, zeolite NaY, and mesoporous material MCM-41

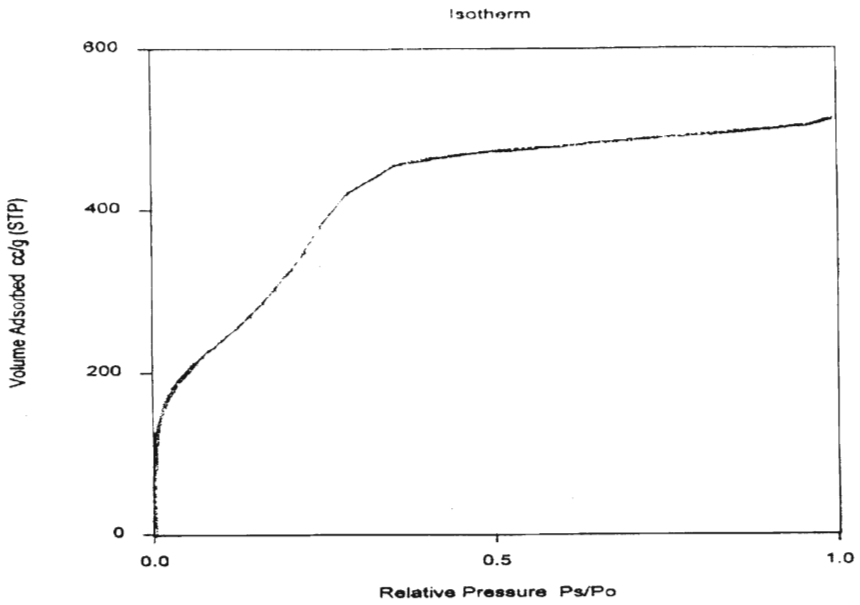


Figure 10a. $N_2$ adsorption-desorption isotherm for Material I (only support, without functional group)

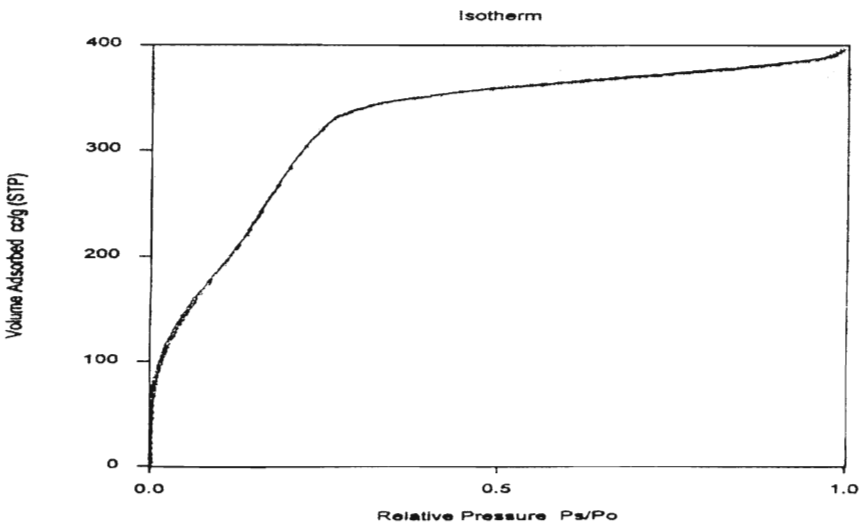


Figure 10b. $N_2$ adsorption-desorption isotherm for Material I (with functional group)

## 3.3 Heavy metal ion adsorption results

### 3.3.1. Loading capacities of $Hg^{2+}$, $Ag^{+}$

As shown in Figure 11, the $Hg^{2+}$ adsorption isotherm for our material indicates quantitative removal of $Hg^{2+}$ ions until saturation was reached at 1.2 mmol/g, or 241 mg/g. This loading capacity is almost an order of magnitude greater than those of functionalized amorphous silica gels.[42,43,44] Thus, the advantage of the crystallized material over the amorphous material as a heavy metal adsorbent has been demonstrated. The hydroxyl groups on the surface of both kinds of material are conducive to the grafting of a very large number of chelating mercaptopropyl groups. But in amorphous silical gel, the irregular pore channels are discontinuous, with narrow pore channels and "ink-bottle" necks susceptible to blockage by the grafted ligand, and hence greatly limiting their potential for the preparation of highly effective adsorbents. In surfactant-templated crystallized material, on the other hand, the uniform pore channels preclude pore blockage by the grafting species, while facilitating the access of metal ions to intergallery adsorption sites, as shown in Figure 12.

The loading capacity of $Ag^{+}$ is around 0.87mmol/g (or, 93.85mg/g), as shown in Figure 13. So the material has stronger adsorption ability for $Hg^{2+}$. From the loading capacity test, we can see that these materials have high adsorption ability for ions if those ions can be adsorbed by the function group on the surface.

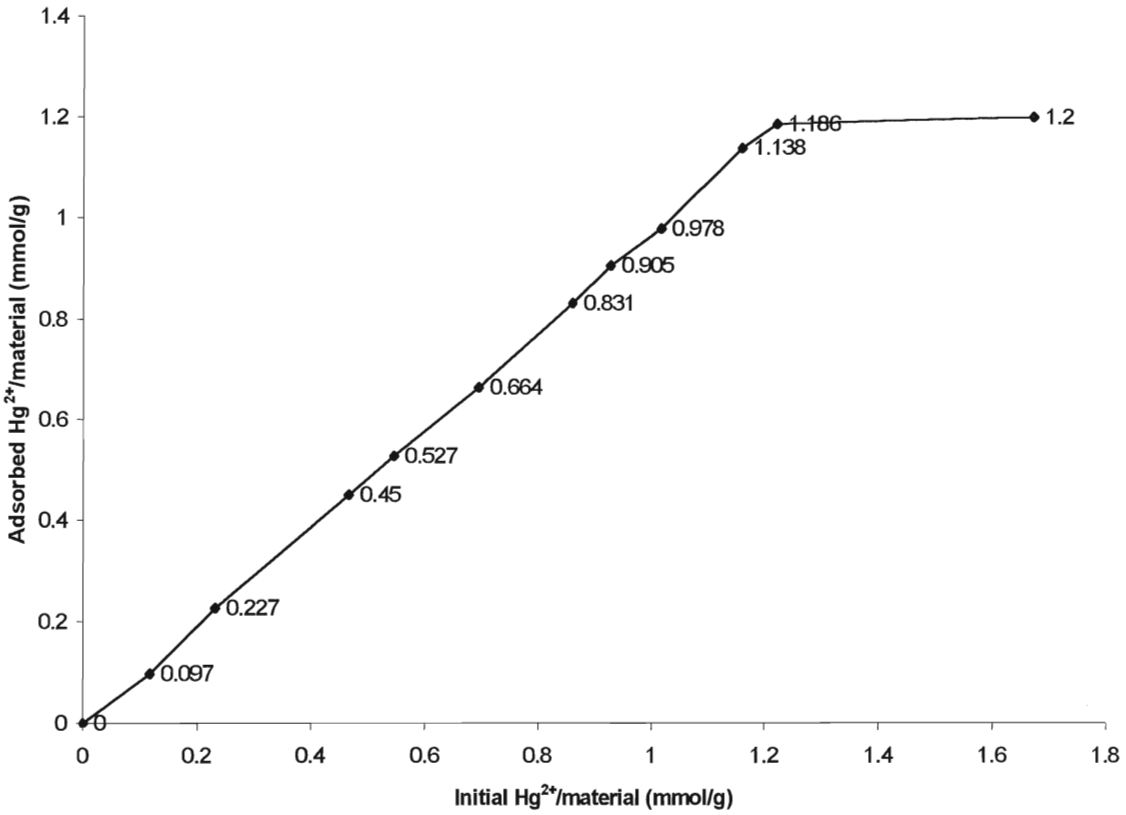


Figure 11. Loading capacity for $Hg^{2+}$

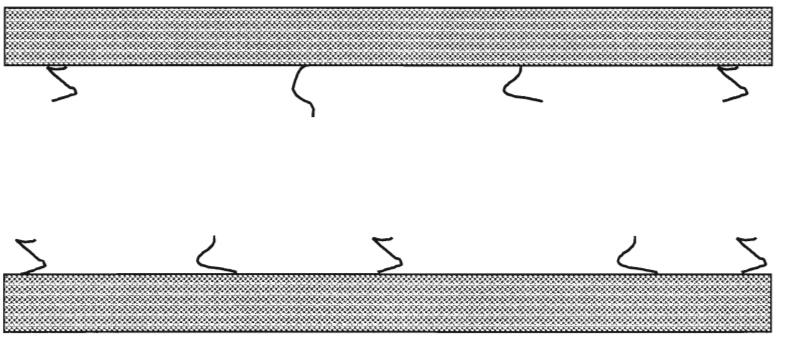

A

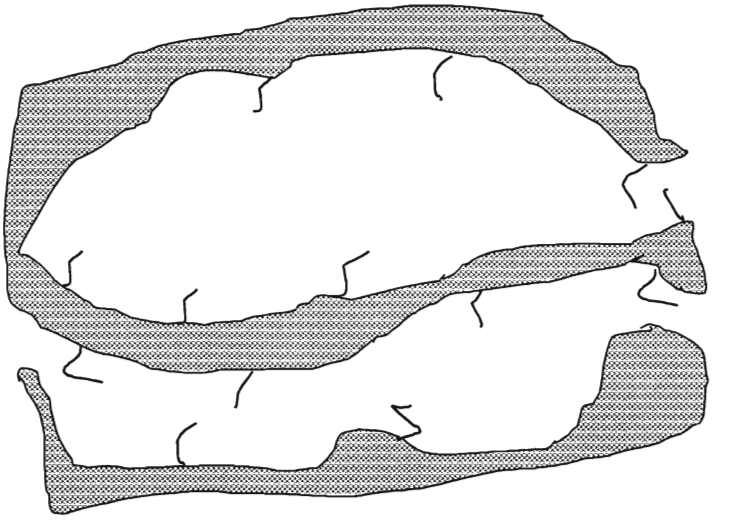

B

Figure 12. A: well-ordered pore channel with grafted function groups
B: amorphous silica with grafted groups

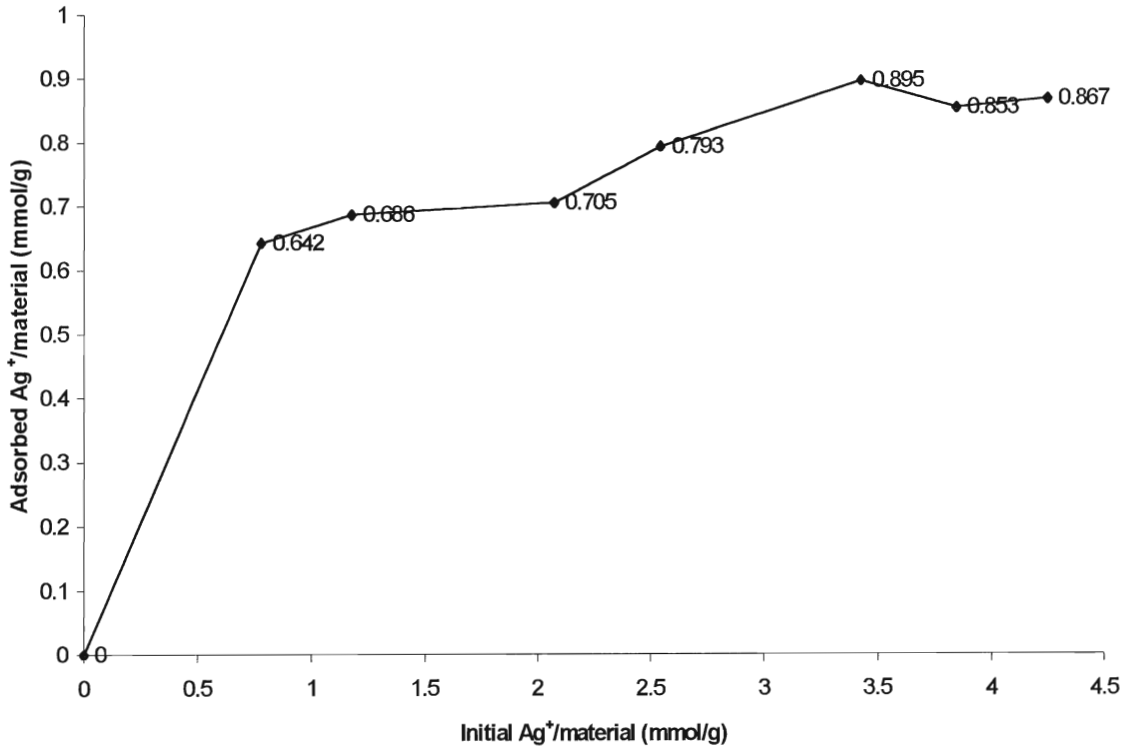


Figure 13. Loading capacity for $Ag^{+}$

### 3.3.2 Batch adsorption of $Pb^{2+}$

$Pb^{2+}$ is another important heavy metal ion. In order to test the adsorption ability for $Pb^{2+}$, a batch adsorption experiment was performed. 10 mg of material was suspended in a 50 mL 1000ng $ml^{-1}$ $Pb^{2+}$ solution. To simulate natural water conditions, the pH of the solution was adjusted to around 5.4. After 30 minutes, the material was filtered off and the $Pb^{2+}$ concentration in the solution was tested. For both of the materials, the resulting $Pb^{2+}$ concentrations were below the detection limit, which was 50 ng $ml^{-1}$. So lead can be well adsorbed by those materials.

### 3.3.3 Batch adsorption of $Cd^{2+}$, $Cu^{2+}$, $Pb^{2+}$, $Hg^{2+}$, $Ag^{+}$ mixture solution

To test the adsorption of a mixture of ions, 10 mg of nanoporous material was added to 50 mL of solution which containing 1000 ng $ml^{-1}$ each of $Cd^{2+}$, $Cu^{2+}$, $Pb^{2+}$, $Hg^{2+}$, $Ag^{+}$. The pH value of the solution was adjusted to 5.0. The adsorption was performed at 10, 20 and 30 minutes' duration. Then the concentrations of those ions were determined after the material was filtered off. The results are shown in Table 2.

Table 2. Concentrations (ng $ml^{-1}$) of ions in solution after different adsorption time (batch adsorption)

| **Material I** | $Hg^{2+}$ | $Ag^{+}$ | $Cu^{2+}$ |
|---|---|---|---|
| 10 minutes | -3.5 | 32.2 | 392 |
| 20 minutes | -13.1 | 24.2 | 328 |
| 30 minutes | -27.6[a], -16[b] | 14.9[a], 17.2[b] | 370[a], 371[b] |
| **Material II** | | | |
| 10 minutes | 42.2 | 28.6 | 355 |
| 20 minutes | 44.1 | 28.1 | 161 |
| 30 minutes | -16.3[a], 28.7[b] | 13.0[a], 13.9[b] | 109[a], 83.9[b] |

a: solution containing only tested ions. b: solution containing 50 μg $ml^{-1}$ $Ca^{2+}$

The concentration of $Cd^{2+}$ and $Pb^{2+}$ remained unchanged after adsorption. The detection limits for $Hg^{2+}$, $Ag^{+}$, $Cu^{2+}$ were 54.9, 52.6 and 60.8 ng $ml^{-1}$, respectively. (calculated by d = blank+$3s_{y/x}$, $s_{y/x}$ is the standard deviation of y-residuals[45]). So, after adsorption, the concentrations of $Hg^{2+}$ and $Ag^{+}$ in the solution were below the detection limit. This experiment suggests that competition occurs between the ions during adsorption. The adsorption ability sequence is: $Hg^{2+} >= Ag^{+} > Cu^{2+} >> Pb^{2+}$ and $Cd^{2+}$.

To test the influence of alkaline earth metal ion, such as occur in hard waters, on the adsorption, another set of tests were done under the same conditions, except that all the solutions also contained 50 μg $ml^{-1}$ $Ca^{2+}$. The results are also shown in Table 2. From the results we can see that the materials have same adsorption ability in the presence of a relatively high concentration of $Ca^{2+}$. So it is possible to use them to collect heavy metal ions in natural hard water, which normally has high levels of $Ca^{2+}$. These results are superior to those for iminodiacetate media, where the presence of Calcium at levels of μg $ml^{-1}$ resulted in poor adsorption.[46]

### 3.3.4 Column adsorption and desorption of $Cu^{2+}$, $Cd^{2+}$, $Pb^{2+}$, $Hg^{2+}$, $Ag^{+}$ mixture

In order to see if the material can be used in a column mode, we did a preliminary experiment. A 50 mL solution, which containing 1000 ng $ml^{-1}$ each of $Cu^{2+}$, $Cd^{2+}$, $Pb^{2+}$, $Hg^{2+}$ and $Ag^{+}$, was prepared. The pH of the solution was adjusted to 5. Then the solution was divided into two 25 mL portions, one portion was determined by ICP-AES directly. The other portion passed through the cartridge which containing 10 mg of Material I at a flow rate of 1 mL $min^{-1}$, prior to determination by ICP-AES. Then 12 mL of 2% $HNO_3$ was passed through the column to elute the ions from the material. The eluate was

collected in a 25 mL volumetric flask, added to line with de-ionized water. The results are listed in Table 3.

Table 3. Concentrations ($ng\ ml^{-1}$) of ions in different solutions (column adsorption)

| **First experiment** | $Hg^{2+}$ | $Ag^{+}$ | $Cu^{2+}$ | $Cd^{2+}$ | $Pb^{2+}$ |
|---|---|---|---|---|---|
| in solution before adsorption | 1210 | 951 | 978 | 901 | 901 |
| in solution passed through Material I (pH=5) | 0.74 | 74.1 | 642 | 875 | 896 |
| in 2% $HNO_3$ eluate from Material I | -83.6 | 49.1 | 310 | 33 | 52.4 |
| **Second experiment** | | | | | |
| in solution passed through Material II (1% HNO3) | 178 | 0.20 | 510 | 975 | 989 |
| in 1% $HNO_3$ eluate from Material II | -66.8 | 0.26 | 24.8 | 5.57 | 22.4 |

To test the influence of the pH on adsorption, we prepared an adsorption solution with 1000ng $ml^{-1}$ of $Cu^{2+}$, $Cd^{2+}$, $Pb^{2+}$, $Hg^{2+}$, $Ag^{+}$, plus 1% (v/v) $HNO_3$. 25 mL of this solution was passed through a column with 10 mg of Material II. Then 25 mL of 1% (v/v) $HNO_3$ was used as eluant. The results are also shown in Table 3.

From these results, we can see the following facts: first, the adsorption for $Hg^{2+}$ and $Ag^{+}$ was very strong, even in 1% (v/v) $HNO_3$ medium. Between 90% and 100% of the ions are adsorbed. That is the good aspect. But they can not be desorbed by 2% (v/v) $HNO_3$. Second, there is almost no adsorption for $Cd^{2+}$ and $Pb^{2+}$. Third, $Cu^{2+}$ is partially adsorbed, and it can be desorbed by 2% (v/v) $HNO_3$, but can not by 1% (v/v) $HNO_3$. Comparing these results to the results from the batch adsorption mode, we can see that the adsorption sequences agree with each other well. So this adsorption difference is not a

random phenomenon. Also, if we look back at the results in batch adsorption test for solution that only contains $Pb^{2+}$ (part 3.3.2), the results are very interesting. $Pb^{2+}$ can be adsorbed well by these materials, if it exists in the solution alone. If $Hg^{2+}$ and $Ag^{+}$ are present in the solution, then the material will not adsorb $Pb^{2+}$. If we count the total mmol of ions in a 25 mL solution that containing 1 $\mu g\ ml^{-1}$ each of $Cu^{2+}$, $Cd^{2+}$, $Pb^{2+}$, $Hg^{2+}$, $Ag^{+}$, it is 1.09 $x10^{-3}$ mmol. The loading capacities for 10 mg of Material I are 12 x $10^{-3}$ mmol for $Hg^{2+}$ at pH 5 and 8.7 x $10^{-3}$ mmol for $Ag^{+}$ at pH 3.5. So it is not likely that the materials did not adsorb $Pb^{2+}$ and $Cd^{2+}$ because of the total amount of ions exceeds the loading capacity. If we think about the ion size, the ionic radii for these ions are listed in Table 4. All the ions are small enough to enter the pore channel, even if they are coordinated to $H_2O$ molecules. If we come to the hard and soft acid and base theory, we can see something. RSH is a soft base; $Hg^{2+}$ and $Ag^{+}$ are soft acids. $Pb^{2+}$ and $Cu^{2+}$ are borderline. As to $Cd^{2+}$, though it is assigned to soft acid category,[47] among the Group IIB elements ($Zn^{2+}$, $Cd^{2+}$, $Hg^{2+}$), $Cd^{2+}$ is more like $Zn^{2+}$,[48] which is borderline. What is more, if we look at their sulfide compounds' solubility product constant $K_{sp}$,[49] we can see something even more interesting: the $K_{sp}$ for HgS and $Ag_2S$ are more than twenty orders of magnitude smaller than those for CdS and PbS. The $K_{sp}$ of CuS is between theses two classes. We can list a sequence for their $K_{sp}$ value: $Hg^{2+} =< Ag^{+} < Cu^{2+} << Pb^{2+} =< Cd^{2+}$. This sequence agrees well with our adsorption sequence result.

Table 4. Ion properties

| | $Hg^{2+}$ | $Ag^{+}$ | $Cd^{2+}$ | $Cu^{2+}$ | $Pb^{2+}$ |
|---|---|---|---|---|---|
| ion radius (A) | 0.83-1.28 (2-8)* | 0.81-1.29 (2-6)* | 0.92-1.45 (4-12)* | 0.71-0.87 (4-6)* | 1.33-1.63 (6-12)* |
| soft, hard acid property | Soft | soft | soft | borderline | borderline |
| sulfide compound $K_{sp}$ | $2 \times 10^{-32}$ (black) $4 \times 10^{-33}$ (red) | $6 \times 10^{-30}$ ($\alpha$ form) $1 \times 10^{-29}$ ($\beta$ form) | $8 \times 10^{-7}$ | $6 \times 10^{-16}$ | $3 \times 10^{-7}$ |

*: the numbers inside the brackets are the corresponding coordination numbers.

It is clear that the micro-scale chemistry between these porous materials and the ions is not simple. It appears that the pore and surface properties of the materials also act as a kind of important "screen". Adsorption results from a co-ordination of the affinity between the ion and the surface function group, and, the "screen effect" of the support material. To find out the exact processes behind this phenomenon we probably need to design other physical chemistry experiments. Which is not the main issue of our work. Our results here suggest other interesting research and application directions for these porous materials. This selective adsorption feature of our materials indicates some profitable application, such as selectively adsorption or recycling of $Hg^{2+}$ and $Ag^{+}$ in the presence of other heavy metal ions. In addition, from the results in the later part of our experiments, we can see that these materials can also used in adsorption of gold.

In order to find out desorption conditions, we prepared $Hg^{2+}$ solutions in two concentration levels. After passing them through columns containing 10 mg of Material II, 5 mL of 30% (v/v) HCl and 5 mL of 3% (m/v) thiourea plus 30% (v/v) HCl were tried

as different desorption solutions. The recoveries for 30% (v/v) HCl were all poor. The recoveries for thiourea plus HCl were good and they are listed in Table 5.

Table 5. Recoveries for $Hg^{2+}$ by using 5 mL of 3% (m/v) thiourea + 30% (v/v) HCl as eluant

| $Hg^{2+}$ solutions passed through column | 20 ng $ml^{-1}$ x 100 mL | 101.5 ng $ml^{-1}$ x 50 mL |
|---|---|---|
| Recovery | 98% ± 14% (n=3) | 110% (n=2) |

### 3.3.5 Adsorption for $Au^{3+}$

Solutions containing 1000ng $ml^{-1}$ $Au^{3+}$ were adsorbed in batch mode for different times. The results are shown in the Table 6.

Table 6. Concentrations of $Au^{3+}$ (ng $ml^{-1}$) in solution after adsorption (batch adsorption)

| | Material I | Material II |
|---|---|---|
| adsorbed after 10 min | 42.1 | 77.9 |
| adsorbed after 30 min | 32.4 | 97.0 |

From the results we can see that more than 90% of $Au^{3+}$ can be adsorbed by the materials within 10 minutes. The detection limit here for gold is 33 ng $ml^{-1}$, so Material I adsorbed almost all the gold ions in the solution. Actually the results could be better than this. While we did this experiment, the serious memory effect problem of $Au^{3+}$ in ICP test has not yet been resolved. A trace amount of $Au^{3+}$ might have remained in the sample introduction system after the measurement of the last (and also the highest concentration) standard solution. After changing to the low concentration sample solution, the apparent

concentration was probably higher than the true value, though we did out best to rinse the sample introduction system between the tests.

We also prepared a 50 mL solution containing 100 ng $ml^{-1}$ of $Au^{3+}$ and a 100 mL solution containing 20 ng $ml^{-1}$ $Au^{3+}$, the pH value of these solution were 3.9. These solutions were passed through cartridges containing 10 mg of Material II at around 1 ml $min^{-1}$. The $Au^{3+}$ concentrations were determined. The results showed less than 2 ng $ml^{-1}$ remained in the solutions. So $Au^{3+}$ can also be well adsorbed by the material in a column mode. 5 mL of 30% (v/v) HCl and 5 mL of 3% (m/v) thiourea plus 30% (v/v) HCl were used as desorption solutions. The recoveries in 30% (v/v) HCl were both lower than 12%. While using 3% (w/v) thiourea plus 30% (v/v) HCl, the recovery for the 20 ng $ml^{-1}$ solution was 86% and the recovery for the 100 ng $ml^{-1}$ solution was 33%.

### 3.3.6 Batch adsorption of $As^{5+}$, $Sb^{5+}$

10 mg of nanoporous material was added to 50 mL of solution which containing 1000 ng $ml^{-1}$ each of As and Sb. The pH of the solution was 5. Adsorption experiments ran for 10, 20 and 30 minutes. The results are shown in Table 7.

Table 7. Batch adsorption results of $As^{5+}$, $Sb^{5+}$

| stirring time (min) | Concentration in solution before adsorption (ng $ml^{-1}$) | | concentration in solutionafter adsorption (ng $ml^{-1}$) | |
|---|---|---|---|---|
| | As | Sb | As | Sb |
| 10 | 1020 | 1010 | 1070 | 233 |
| 20 | | | 1080 | 210 |
| 30 | | | 1050 | 211 |

From the results we can see that there is no adsorption of $As^{5+}$ and there is a 80% adsorption of $Sb^{5+}$. There is no obvious difference between 20 minutes and 30 minutes' adsorption for $Sb^{5+}$.

### 3.3.7. Adsorption for $CH_3HgCl$

Methylmercury is an extremely toxic material. To extend the application of our materials, we added 10 mg of each of the two materials into solutions containing 1000 ng $ml^{-1}$ of $CH_3HgCl$. The adsorption results are listed in Table 8. From the results we can see that 90% of the $CH_3HgCl$ can be adsorbed in 10 minutes.

Table 8. Concentrations of $CH_3HgCl$ (ng $ml^{-1}$) in solutions after adsorption (batch adsorption)

| | Material I | Material II |
|---|---|---|
| adsorbed after 10 min | 99 | 116 |
| Adsorbed after 30 min | 93 | 128 |

An interesting thing we should mention here is that the pH value of the adsorption solution was 2.8. So, the adsorption of $CH_3HgCl$ is strong and it is obviously better than amine containing complexing agents, whose complexing ability obviously depends on pH. If we look at the results in Table 3 (second experiment), we can find that inorganic mercury can be adsorbed even in 1% (v/v) $HNO_3$ medium. This might suggest some possibility for the speciation of inorganic mercury and organic mercury at different pH during adsorption or desorption.

Column adsorption-desorption experiments were also performed. $CH_3HgCl$ solutions were prepared in two concentration levels at pH 3 to 4. After passing them

through columns containing 10 mg of Material II, 5 mL of 30% (V/V) HCl and 5 mL of 3% (m/v) thiourea plus 30% (v/v) HCl were tried as different desorption solutions. The recoveries for 30% (v/v) HCl were all not ideal. The recoveries for thiourea plus HCl were good and they are listed in Table 9.

Table 9. Recoveries for $CH_3HgCl$ by using 5 mL of 3% (m/v) thiourea + 30% (v/v) HCl as eluant

| Different $CH_3HgCl$ solutions passed through column | 18 ng $ml^{-1}$ x 100 mL | 143.8 ng $ml^{-1}$ x 50 mL |
|---|---|---|
| Recovery | 88% ± 1% (n=3) | 92% (n=2) |

# 4. Results and discussion for memory effect study

In our memory effect study, we applied the following experiment procedure to obtain our results: To obtain washout curves, a blank solution containing the appropriate complexing agent and 1% (v/v) nitric acid, was aspirated into the plasma followed by a solution containing analyte and complexing agent. After sufficient time had been allowed for a steady signal to be established, the blank solution was reintroduced into the system.

## 4.1. Criteria for wash-out time

The definition of wash-out time, defined by Varnes[34] as the time required for the analytical signal to go from the first significant decline to a 99.9% reduction is useful provided the sample signal is relatively low. When samples of high concentration are introduced, however, a reduction of 99.9% of the steady-state signal produces a resultant signal that is not sufficiently close to the baseline if the sample is followed by another

whose analyte concentration is low. Although preliminary screening will minimize such eventualities, the process is needlessly time-consuming, if it can be avoided. In such cases, the washout time should measure the time required for the sample signal to be reduced to the baseline signal. Using the mean blank signal plus three times its standard deviation gives an appropriate estimate of the point at which the analyte can be assumed to have been washed out. The results of experiments reported in this work show that, when low analyte concentrations are used, it takes longer for the sample signal to be reduced by 99.9% than it does to fall within $3\sigma$ of the mean blank signal. Once the signal falls within the $3\sigma$ envelope, even though there remains a small determinate error, this criterion gives a more reasonable measure of wash-out than the 99.9% reduction of the steady-state signal. Thus, the results reported in this thesis use both criteria for evaluating washout times. Varnes' 99% criterion for the wash-in time appears quite reasonable,[34] as long as there are no memory effects that delay the onset of the steady-state signal.

## 4.2 Observations of memory effect problems

In order to evaluate the performance of the nebulizer-spray chamber with respect to wash-in and wash-out behaviour, a series of experiments was performed that illustrate clearly the problematic areas of sample introduction. Solutions containing several elements, including ruthenium were investigated. Ruthenium is an element that does not have a problematic washout time. A sample containing 500ng $ml^{-1}$ of $Ru^{3+}$, 1μg $ml^{-1}$ of $Hg^{2+}$ and 1% (v/v) $HNO_3$ was introduced into the plasma. Figures 14a and 14b shows the signals of the wash-in and wash-out for the two elements. While the ruthenium signal reached the steady signal within seconds, the mercury signal required more than 12

minutes to reach the steady state criterion. The ruthenium signal fell to the 99.9% reduction line rapidly (41 seconds) after reintroduction of the blank, while the mercury signal took approximately 17.5 minutes to fall within 3σ of the mean blank signal and more than 19.5 minutes to achieve a 99.9% reduction in the sample signal. This experiment demonstrates that a prodigious amount of time is required between samples when determinations of elements with long wash-out times are attempted. Ruthenium determinations could be carried out with a delay of only seconds between the rinse step and the introduction of a new sample, whereas mercury samples could be introduced with a delay of at least 20 minutes between samples.

For some elements that exhibit problematic washout times, the situation is further complicated by long wash-in times. Figures 15a and 15b show the results of the wash-in time observed for gold. Presumably, gold is adsorbed onto the walls of the sample introduction system during the initial period of introduction, which results in a sigmoidal shape to the initial signal and a wash-in time of almost 12 minutes. Like mercury, the washout time for gold in a 1% (v/v) nitric acid solution is unacceptably long, as seen in Figure 15b. In fact, the time required for the signal to fall within 3σ of the mean blank signal exceeded 30 minutes, and the time required for a reduction of 99.9% of the signal was significantly longer and was not determined because of the length of time required for the experiment.

Silver is washed out more quickly than gold or mercury. However, the time required for the signal to fall within three σ of the blank signal (approximately 7 minutes) is still much greater than times for elements without memory effects, such as ruthenium. The wash-out curve of silver in a 1% nitric acid solution is shown in Figure 16.

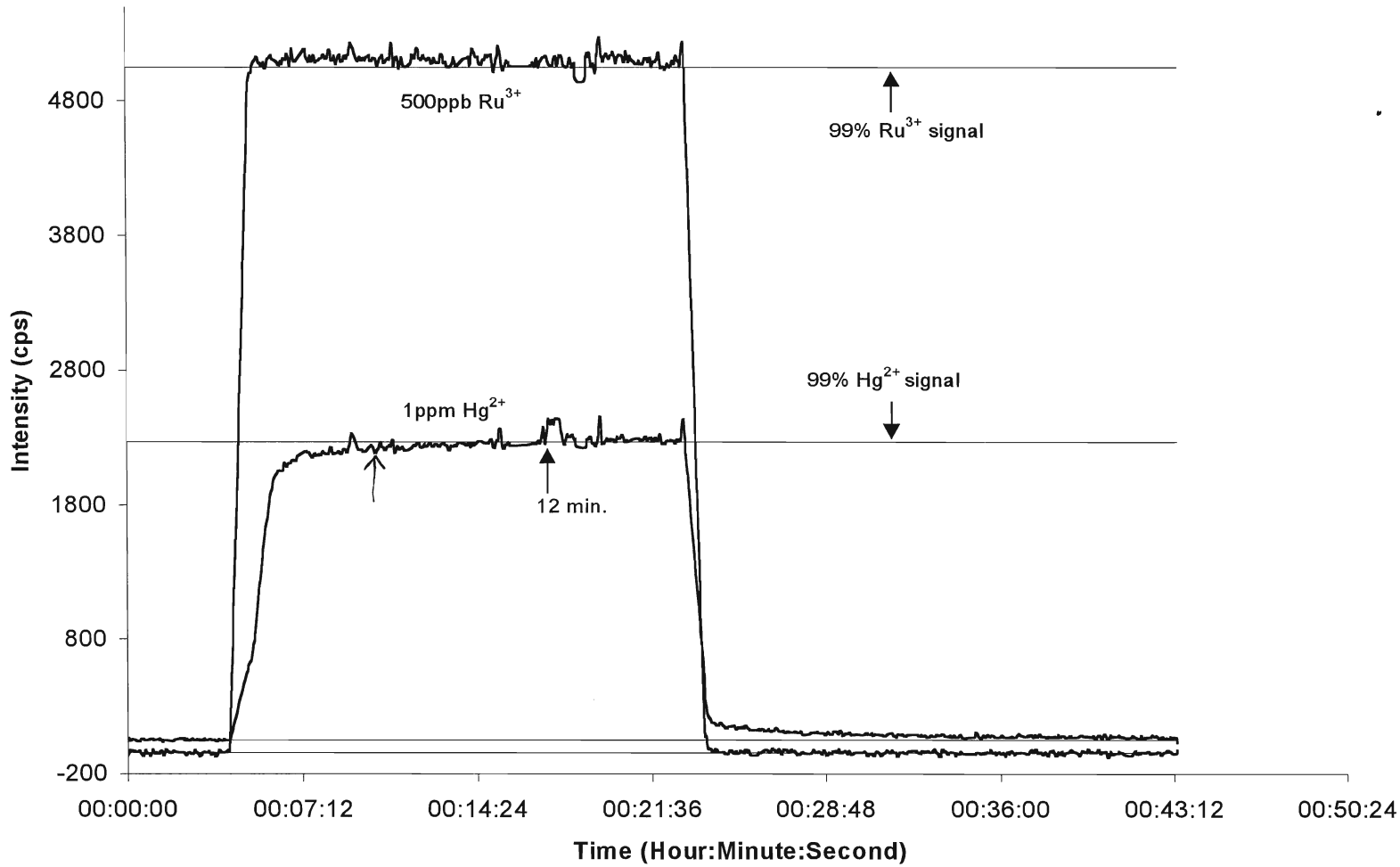


Figure 14a. 1 μg $ml^{-1}$ $Hg^{2+}$ and 500 ng $ml^{-1}$ $Ru^{3+}$ in 1% (v/v) $HNO_3$

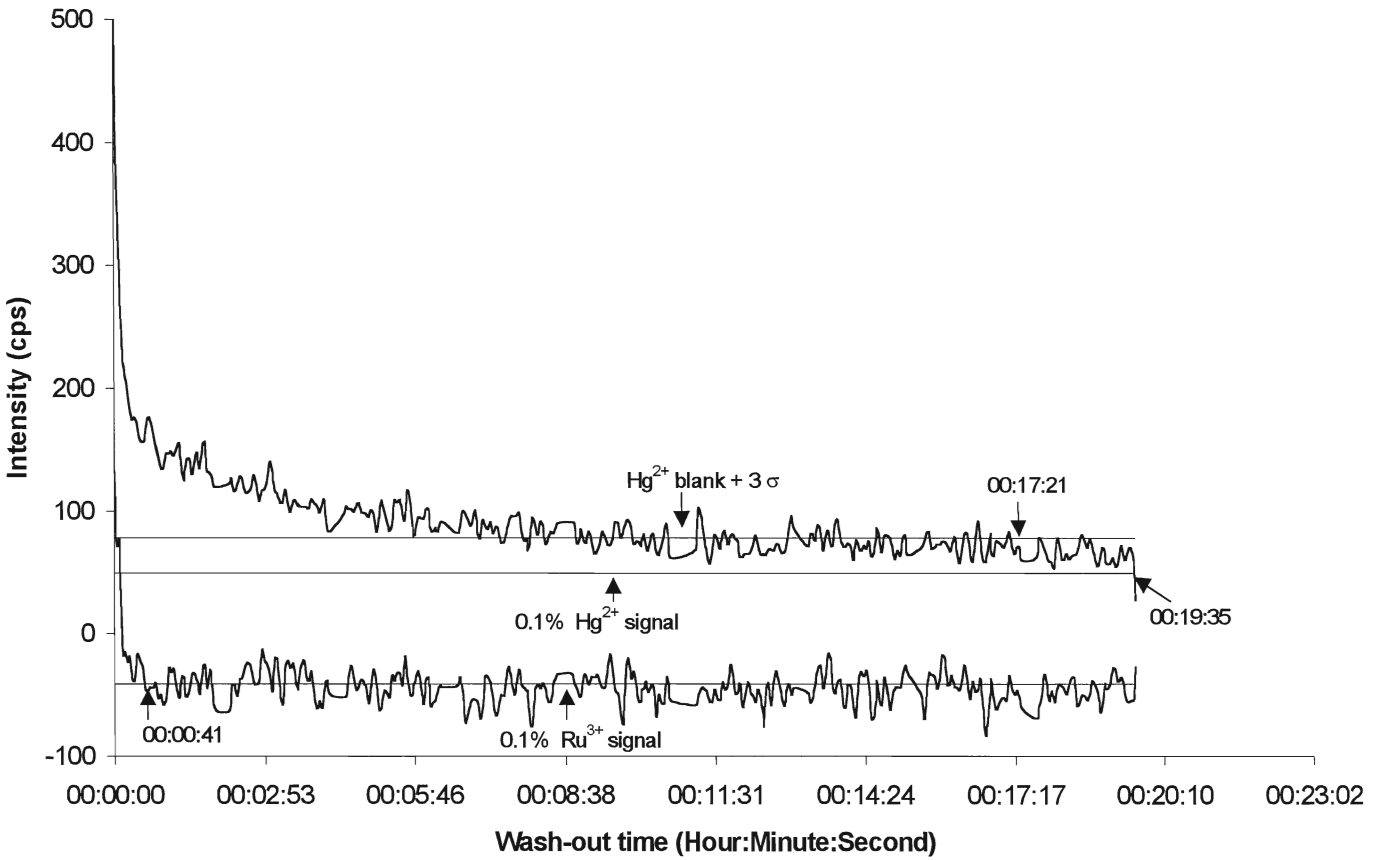


Figure 14b. 1 μg ml$^{-1}$ $Hg^{2+}$ and 500 ng ml-1 $Ru^{3+}$ in 1% (v/v) $HNO_3$

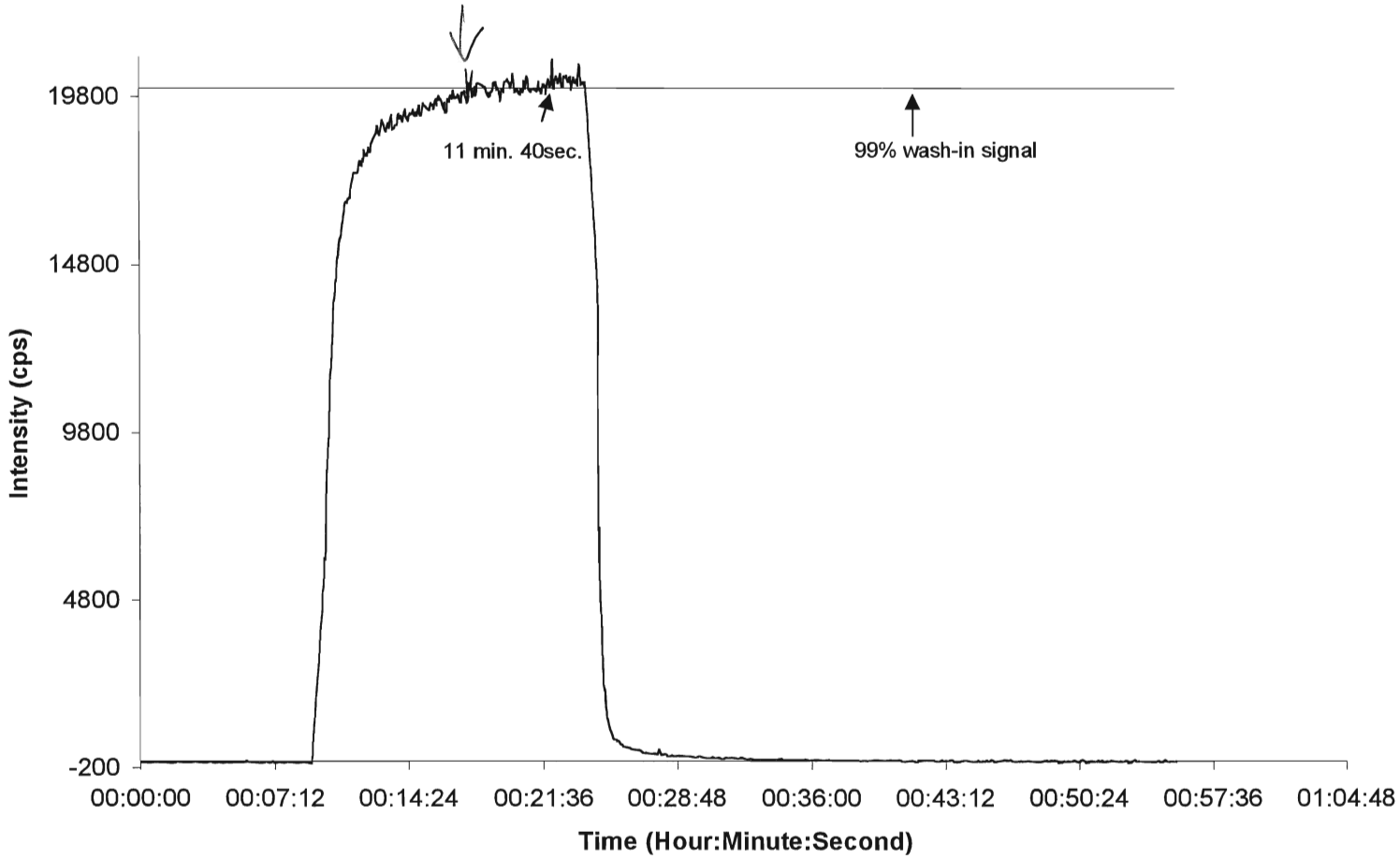


Figure 15a. 1μg $ml^{-1}$ $Au^{3+}$ in 1% (v/v) $HNO_3$

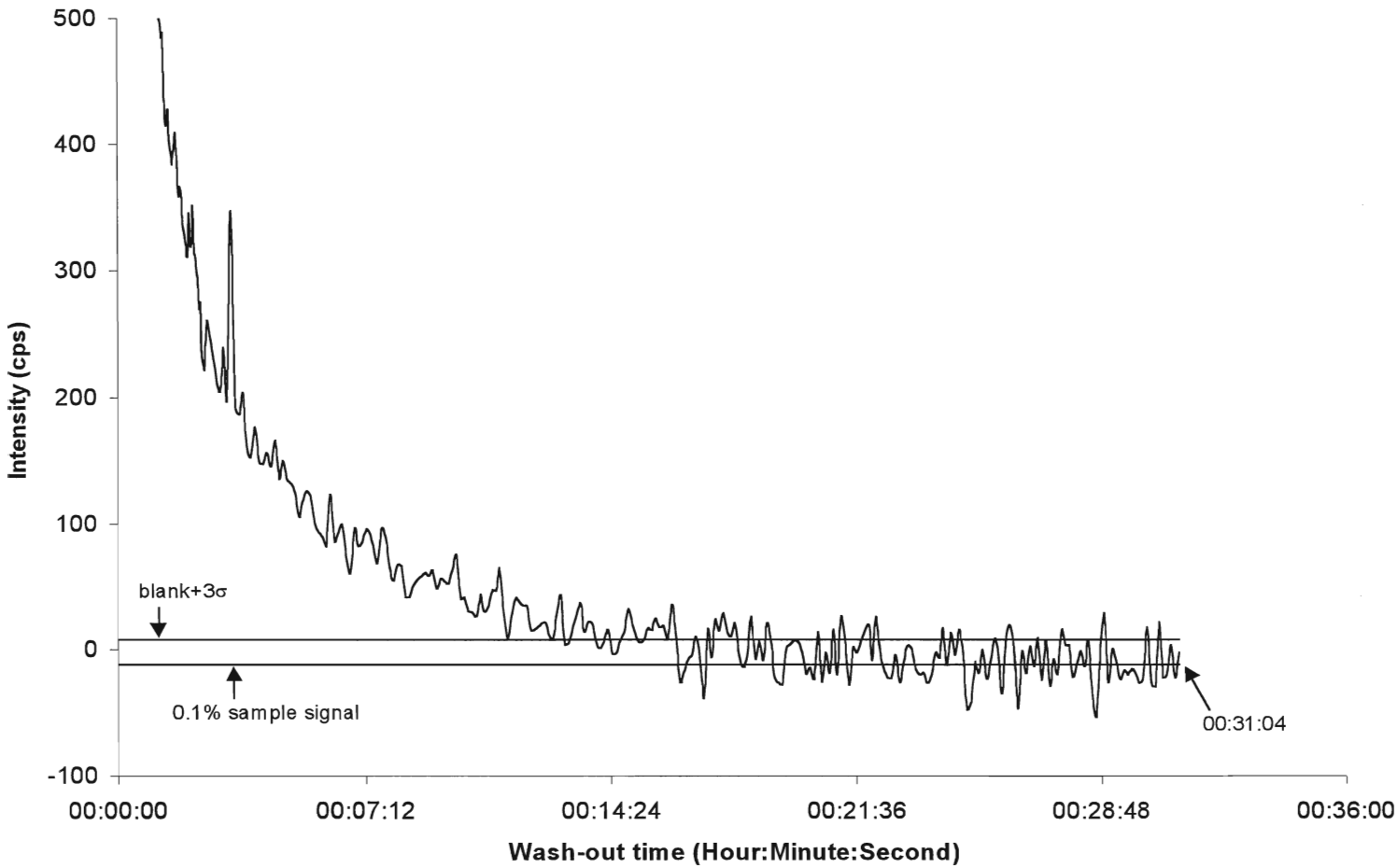


Figure 15b. 1μg $ml^{-1}$ $Au^{3+}$ in 1% (v/v) $HNO_3$

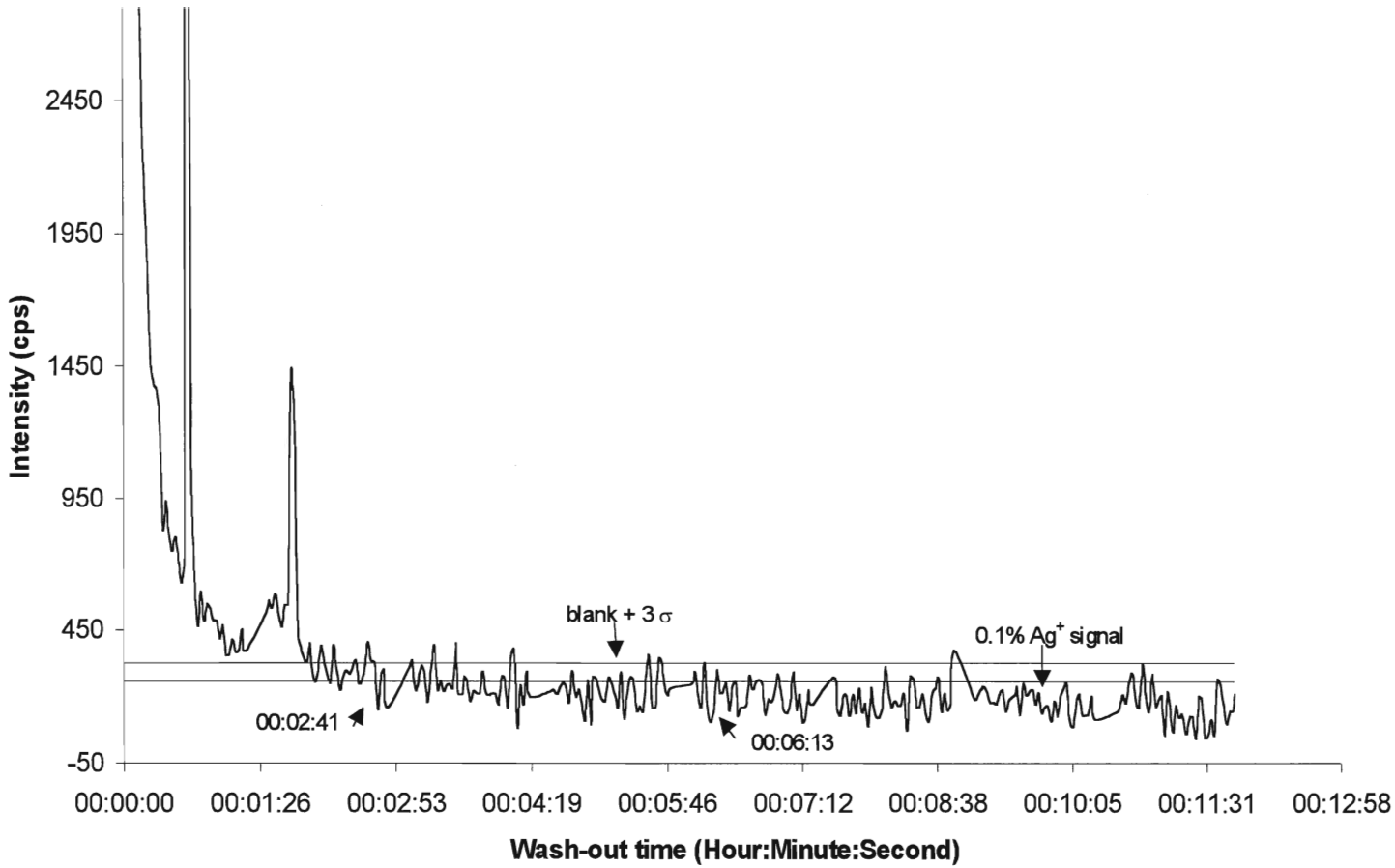


Figure 16. 1μg $ml^{-1}$ $Ag^{+}$ in 1% (v/v) $HNO_3$

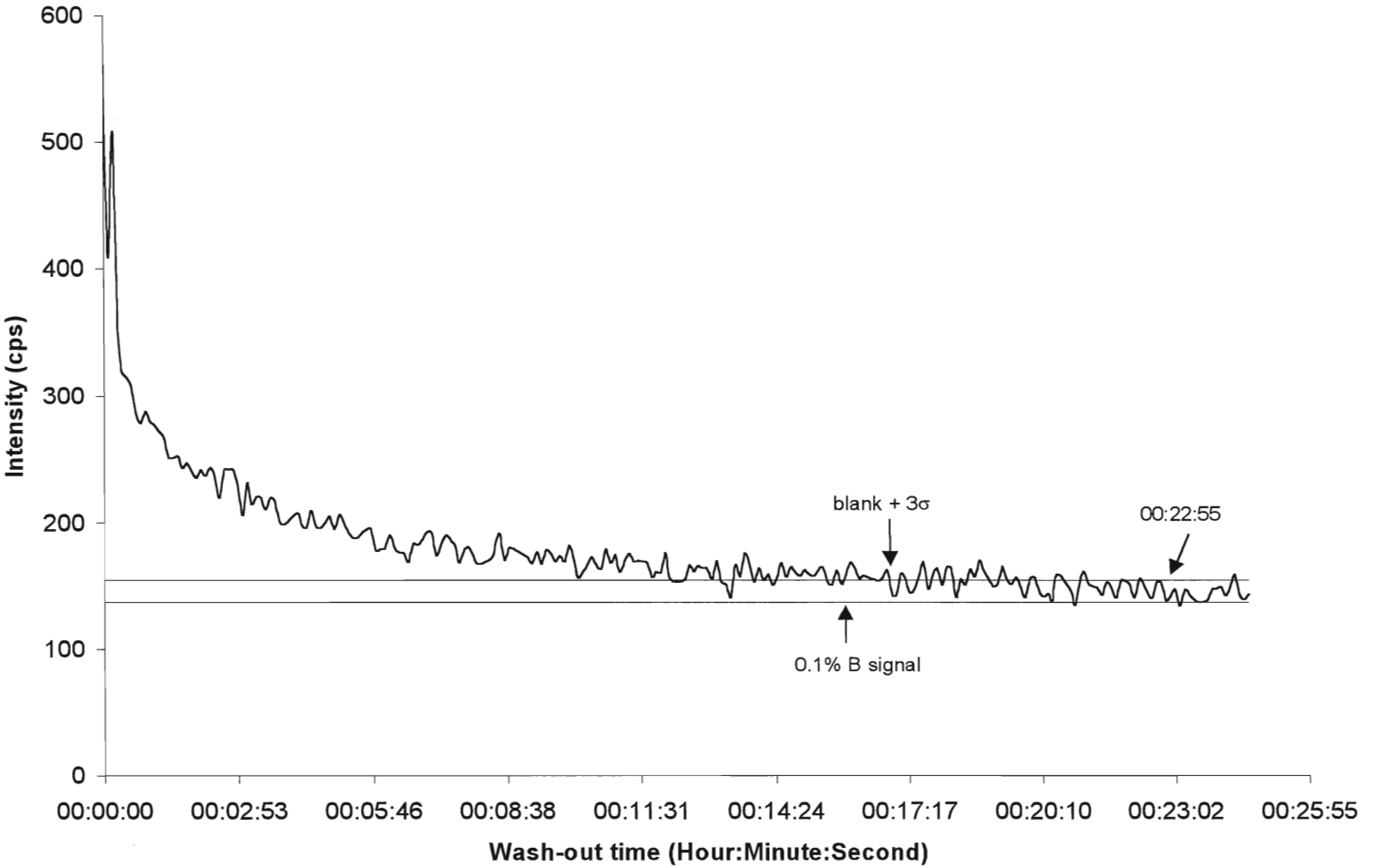


Figure 17. 1 μg $ml^{-1}$ B in 1% (v/v) $HNO_3$

Boron differs from the other three elements in that it exists as a molecular species in solution. The processes involved in preventing boron from washing out quickly are likely different than those responsible for the memory effects of mercury, silver and gold. An argument could be made that the interactions of boric acid with the borosilicate glass components of the introduction system are primarily responsible for the long washout times exhibited by boron. However, the fact that long washout times are observed even when all components of the introduction system are made from plastic, suggests that the problem is more complex. A 1% (v/v) nitric acid solution containing 1 μg $ml^{-1}$ boron, required 10-24 minutes of washing to decrease the sample signal to within 3σ of the mean blank signal. A 99.9% reduction in sample signal occurs after more than 20 minutes, as shown in Figure 17.

## 4.3. Elimination of memory effects for mercury, gold and silver

The use of HBr to eliminate memory effects of mercury has been reported, as described in the introduction. In an attempt to replicate these results, a solution of 1% (v/v) HBr was used to obtain the baseline which was then followed by injection of a 1μg $ml^{-1}$ mercury solution. The blank solution was introduced again and the signal intensities recorded. The curves obtained are shown in Figures 18a and 18b. The time required for the signal to fall within 3σ of the mean blank signal decreased from 17.5 minutes to 8.75 minutes and the time required for a disappearance of 99.9% of the signal decreased from greater than 19.5 minutes to less than 19.5 minutes. Nevertheless, the washout time remains unacceptably long for routine analyses. In addition, Figure 18a shows a longer wash-in time of almost 5 minutes for mercury in the HBr matrix, further limiting the

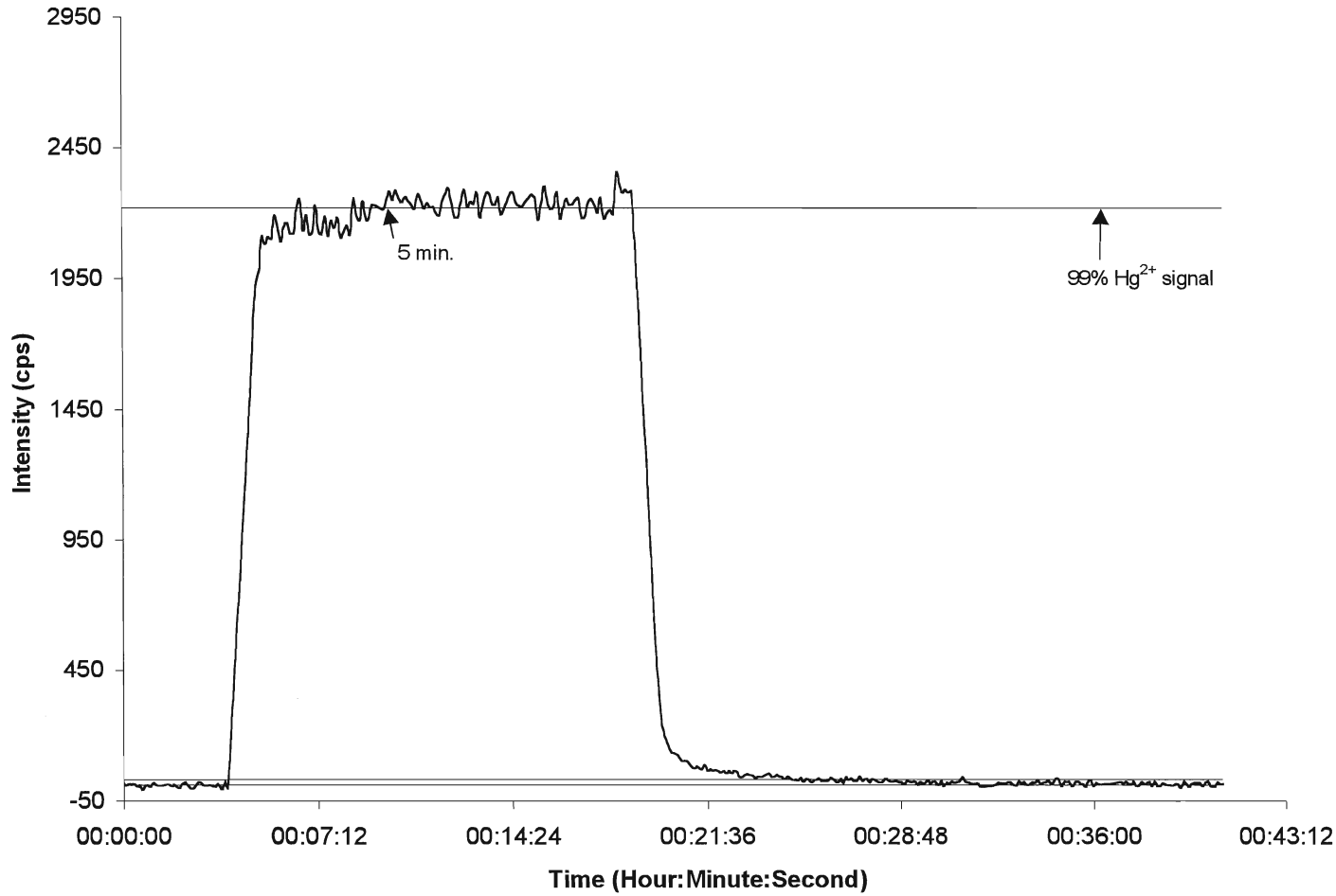


Figure 18a. 1 μg $ml^{-1}$ $Hg^{2+}$ in 1% (v/v) HBr

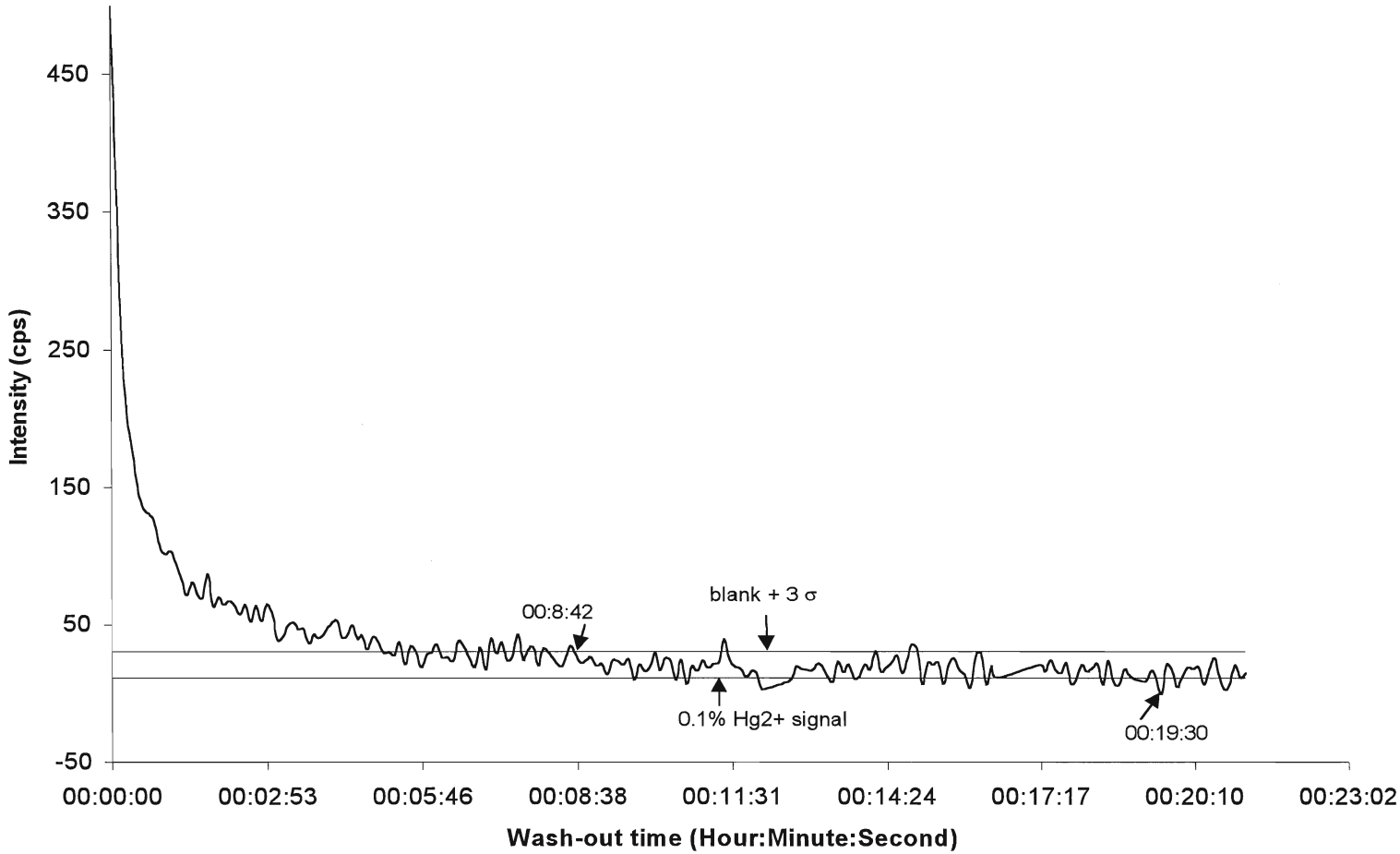


Figure 18b. 1 μg $ml^{-1}$ $Hg^{2+}$ in 1% (v/v) HBr

applicability of the HBr matrix for minimizing the mercury memory effect. The use of a 1% (v/v) HBr solution was also explored for the elimination of memory effects for gold. No improvement in washout time was observed.

It was thought that the use of a complexing agent might be useful in minimizing memory effects of the three transition metals, the assumption being that such an agent would prevent interactions between the analyte and the surface area of the introduction system. Although some analysts use detergents to wet surfaces, and therefore enhance a smoother release of analytes from the surface, the behaviour of the elements under review are anomalous and therefore their memory effect is unlikely to be remedied by such a technique, which seeks to minimize beading on the surface of the spray-chamber. Ligands containing sulfur atoms were predicted to have a favorable affect on the washout times of the analytes of interest. Sulfur containing ligands, being soft Lewis bases, would be preferred ligands for co-ordination to soft Lewis acids, such as mercury, gold and silver. In addition, such co-ordinated sulfur species would be less susceptible to decomposition in acid solutions typically used to maintain analytes in solution. A solution containing 2% (m/v) L-cysteine, 1% (v/v) nitric acid, 1 μg $ml^{-1}$ $Hg^{2+}$ and 500ng $ml^{-1}$ $Ru^{3+}$ as well as a blank solution containing 2% (m/v) L-cysteine and 1% (v/v) nitric acid were prepared and used to determine the washout time of mercury. The results, shown in Figure 19a and 19b, demonstrate that, under these conditions, mercury has a washout time of less than 30 seconds and is comparable to that of ruthenium.

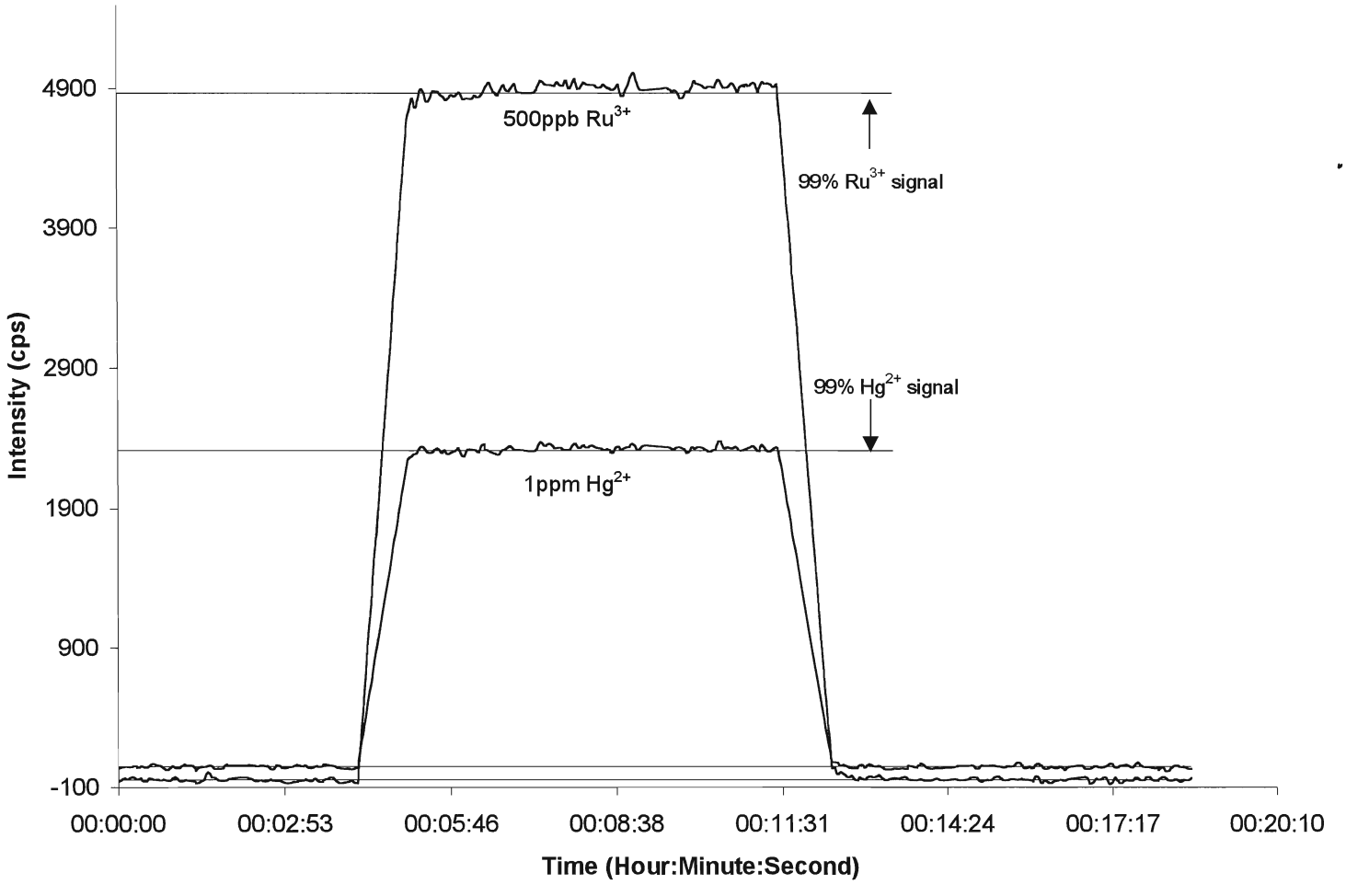


Figure 19a. 1 μg $ml^{-1}$ $Hg^{2+}$, 500 ng $ml^{-1}$ $Ru^{3+}$ in 2% (m/v) L-cysteine and 1% (v/v) $HNO_3$

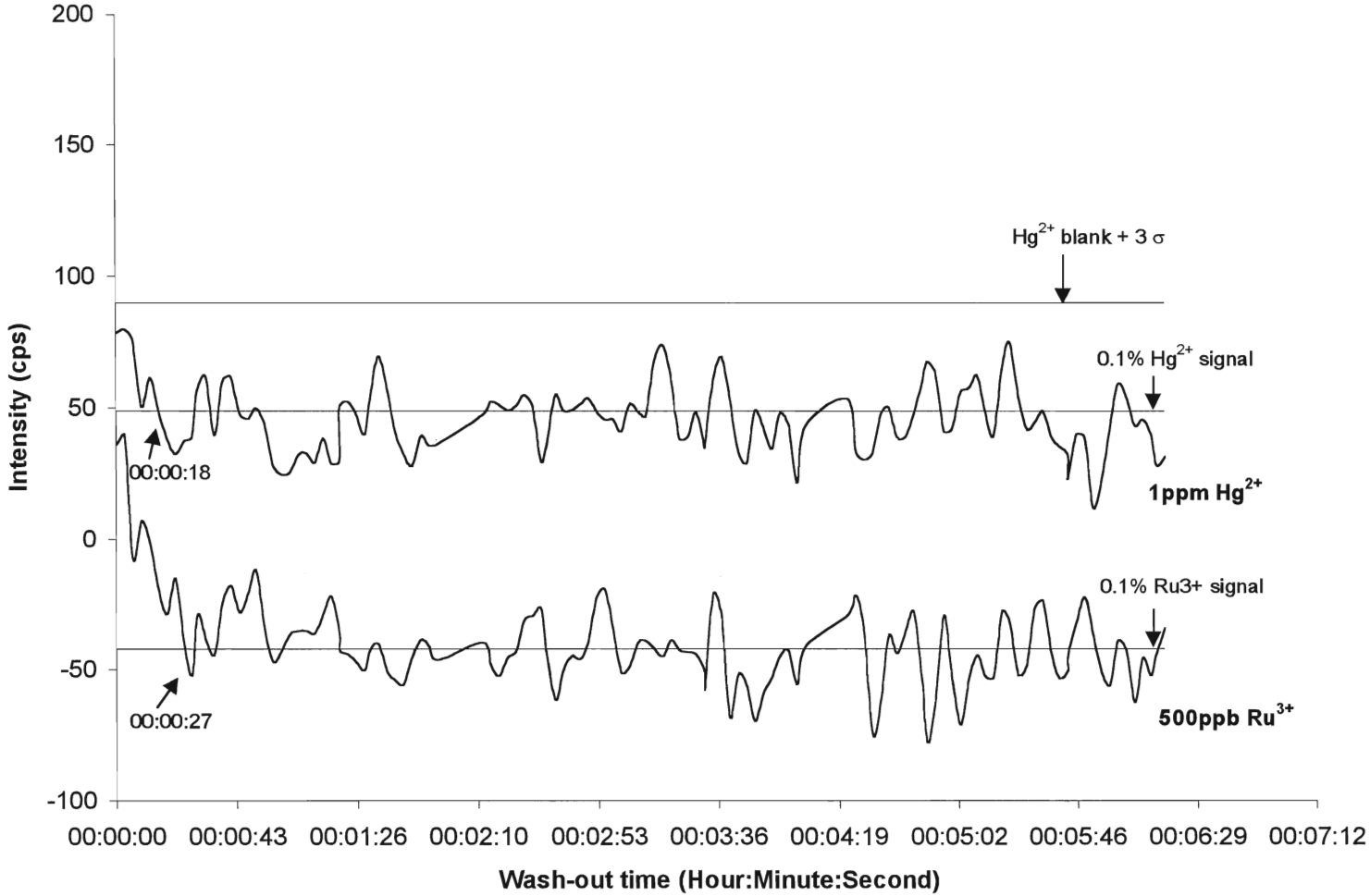


Figure 19b. 1 μg $ml^{-1}$ $Hg^{2+}$, 500 ng $ml^{-1}$ $Ru^{3+}$ in 2% (m/v) L-cysteine and 1% (v/v) $HNO_3$

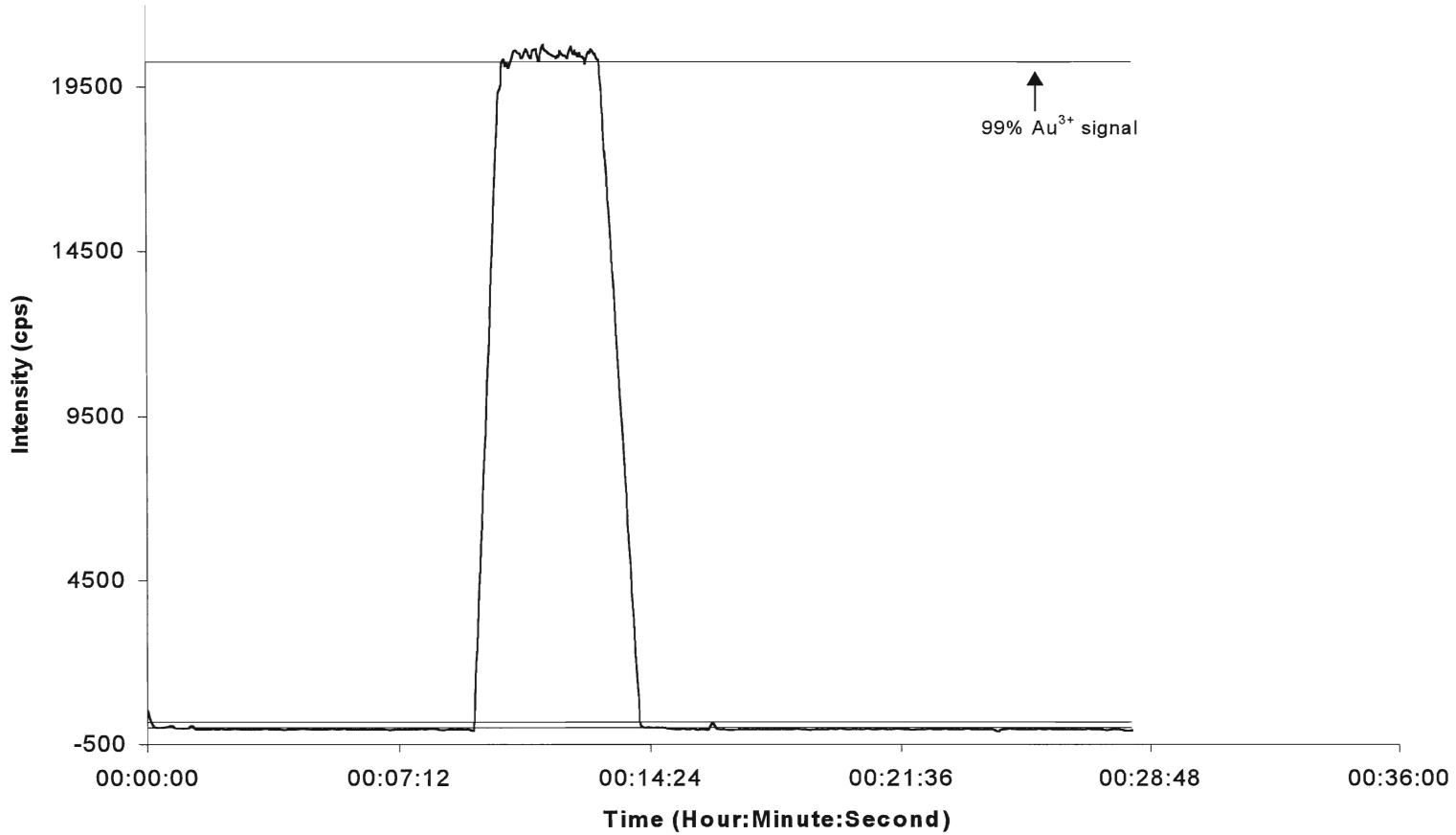


Figure 20a. 1 μg $ml^{-1}$ $Au^{3+}$ in 2% (m/v) L-cysteine and 1% (v/v) $HNO_3$

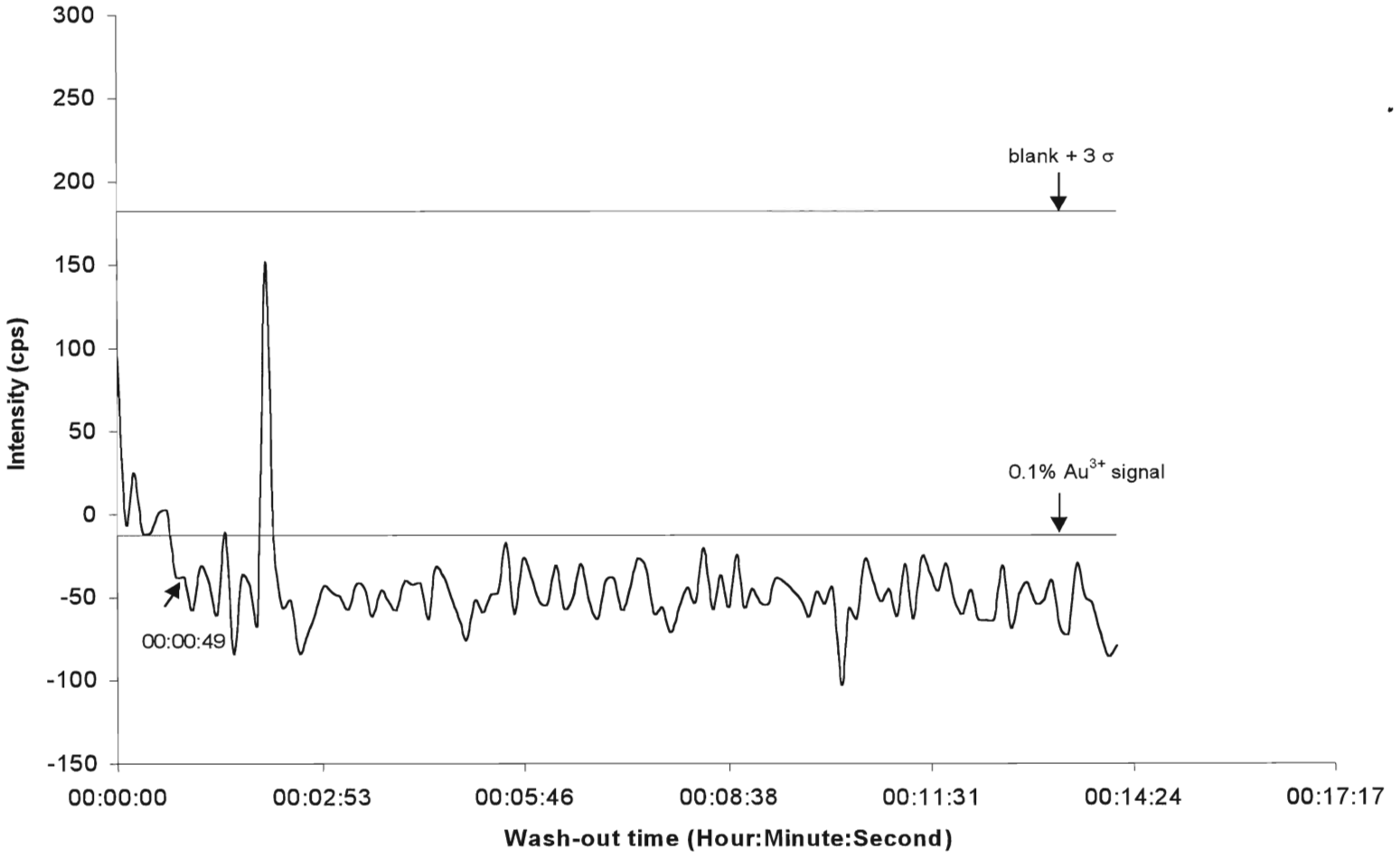


Figure20b. 1 μg $ml^{-1}$ $Au^{3+}$ in 2% (m/v) L-cysteine and 1% (v/v) $HNO_3$

A similar experiment was designed for investigation of the gold memory effect. As shown in Figures 20a and b, a 1μg $ml^{-1}$ $Au^{3+}$ solution containing 2% (m/v) L-cysteine and 1% (v/v) nitric acid delivered a wash-out time of less than 50 seconds using both the 3σ and the 0.1% of the steady-state signal criteria. Comparison of Figures 19a and 20a with Figure 14a and 15a clearly illustrates that the memory effects of mercury and gold, at low concentrations, are eliminated by adding 2% (m/v) L-cysteine to the acidified sample solution.

Contrary to the results obtained with mercury and gold, the addition of 2% (m/v) L-cysteine to a 1μg $ml^{-1}$ $Ag^{+}$ solution containing 1% (v/v) nitric acid resulted in an increase of 12 minutes in the time required for the loss of 99.9% of the sample signal. A possible explanation for this result is that L-cysteine reduced $Ag^{+}$ to $Ag^{0}$, while being itself oxidized to L-cystine. A second complexing agent, L-histidine, which contains pyrazine rather than a sulfur group, was tested with limited success. The sample signal fell within 3σ of the mean blank signal after 3-5 minutes. The memory effect problem for silver was completely resolved, however, by the addition of 1% (m/v) thiourea, another sulfur containing ligand, to a solution containing 1μg $ml^{-1}$ $Ag^{+}$ and 1% (v/v) nitric acid. The sample signal was reduced by 99.9% in 1.25 – 1.5 minutes, and fell within 3σ of the blank signal in less than 1.75 minutes.

The mining industry often requires determination of high concentrations of mercury and gold. In order to test the effectiveness of L-cysteine as a complexing agent for high concentrations of these elements, a solution containing 100μg $ml^{-1}$ $Au^{3+}$, 100μg $ml^{-1}$ $Hg^{2+}$, 2% (m/v) L-cysteine, 1% (v/v) HCl and 0.3% (v/v) nitric acid was prepared. The acid mixture was used to duplicate conditions where sample digestion is carried out

using aqua regia. L-cystine, formed by the oxidation of L-cysteine, precipitated immediately after mixing, compromising the ability of the nebulizer to effectively deliver a consistent flow of aerosol. The reduction of the analytes, made evident by the prolonged memory effect described above for silver, as well as by the precipitation of L-cystine, suggests that analytes at high concentrations may be precipitated from solution by the reduction reaction. In order to retain the benefits of the sulfur-containing ligand, without the problems of precipitation of the reagent, L-cysteine was replaced by 1-2% thiourea. Both gold and mercury required less than 45 seconds for a 99.9% reduction of analyte signal. As demonstrated in Figures 21a-22b, the analyte signal fell within $3\sigma$ of the blank signal in less than 3.5 minutes for gold, and less than 2 minutes for mercury. Recognizing that real samples necessarily contain a more complex matrix, a solution containing 100$\mu$g $ml^{-1}Au^{3+}$, $Hg^{2+}$, $Zn^{2+}$, $Cu^{2+}$, $Al^{3+}$, $Mg^{2+}$, $K^{+}$, $Fe^{3+}$, 1000 $\mu$g $ml^{-1}$ $Ca^{2+}$, Mg and $Na^{+}$, 2% (m/v) thiourea and 1-2% (v/v) nitric acid was prepared. Again, the analyte signals were reduced to within $3\sigma$ of the blank signal in less than 3.5 minutes for gold and less than 2 minutes for mercury. Though clear when prepared, the solution became cloudy after 3-4 hours. Thus, it is necessary for high concentration solutions to be prepared just prior to analysis. Solutions containing 2% (m/v) thiourea, 1-2% (v/v) nitric acid and concentrations of 10, 50 and 100 $\mu$g $ml^{-1}$ of the ten elements listed above were used to obtain calibration data. The correlation coefficients of 0.9999 for the mercury line at 194.168nm and 1.0000 for the gold line at 242.795nm show the method to be useful for quantitative analyses.

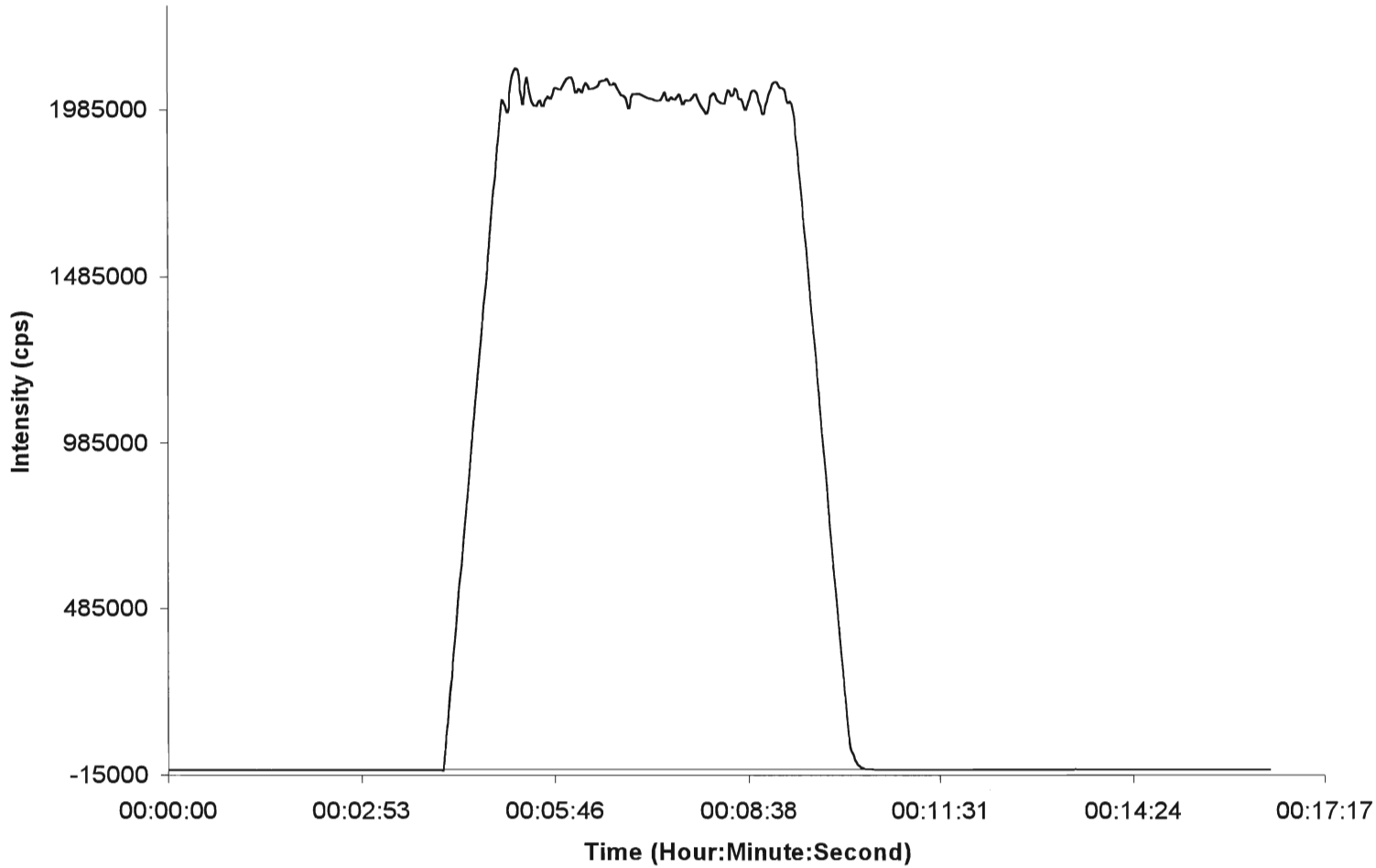


Figure 21a. 100 μg $ml^{-1}$ $Au^{3+}$ in 1% (m/v) thiourea, 1% (v/v) HCl and 0.3% (v/v) $HNO_3$

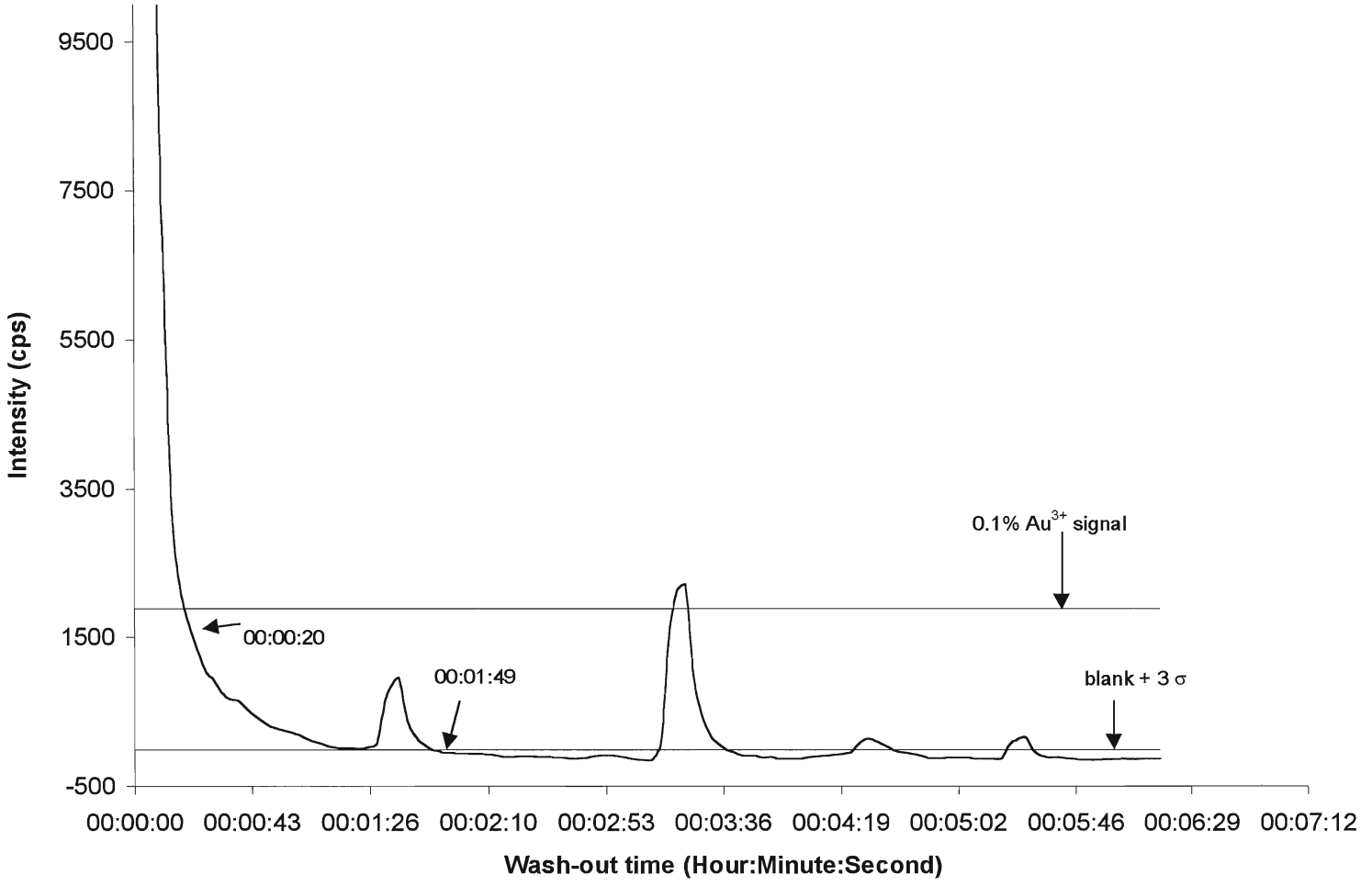


Figure 21b. 100 μg $ml^{-1}$ $Au^{3+}$ in 1% (m/v) thiourea, 1% (v/v) HCl and 0.3% (v/v) $HNO_3$

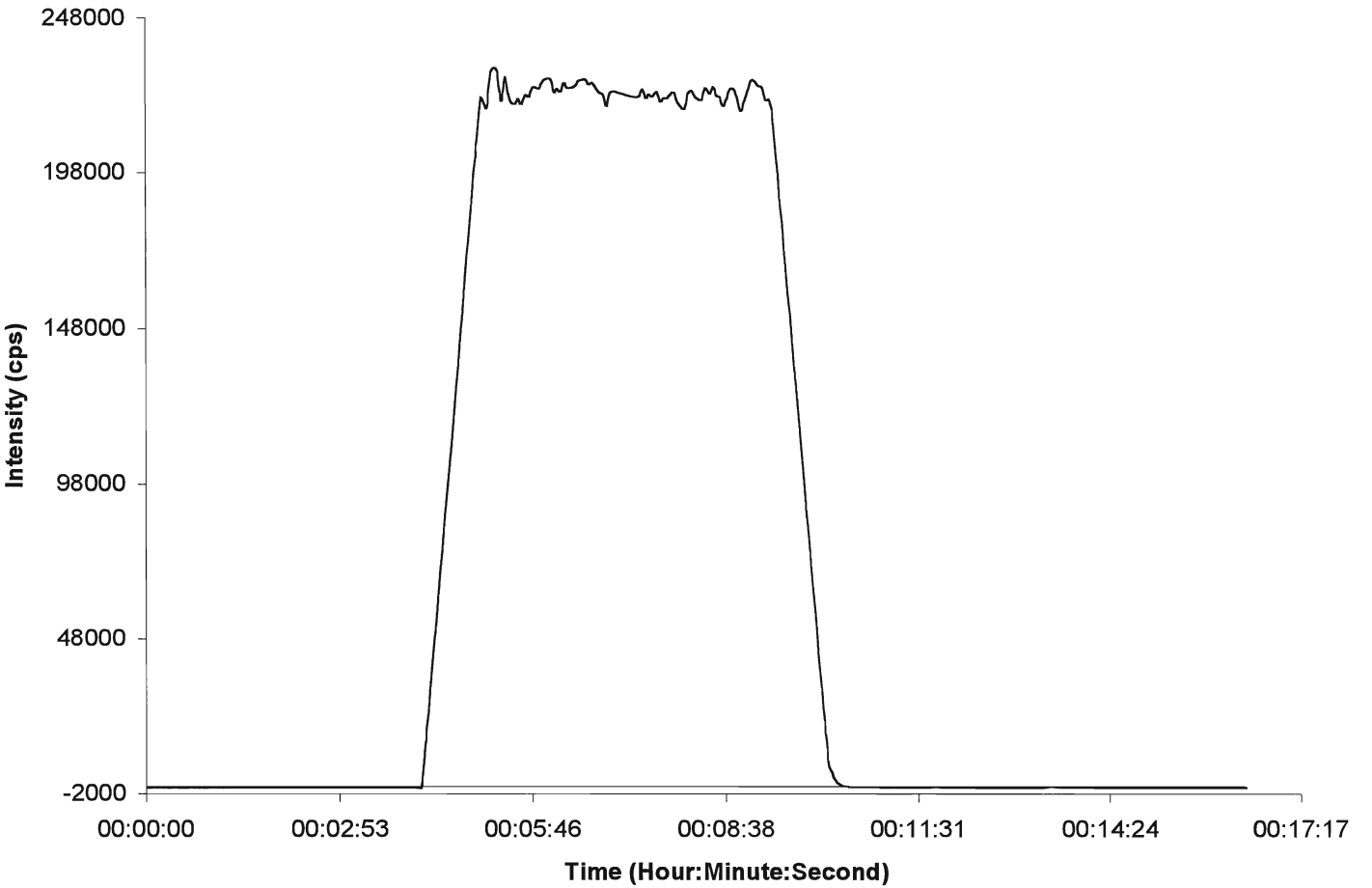


Figure 22a. 100 μg $ml^{-1}$ $Hg^{2+}$ in 1% (m/v) thiourea, 1% (v/v) HCl and 0.3% (v/v) $HNO_3$

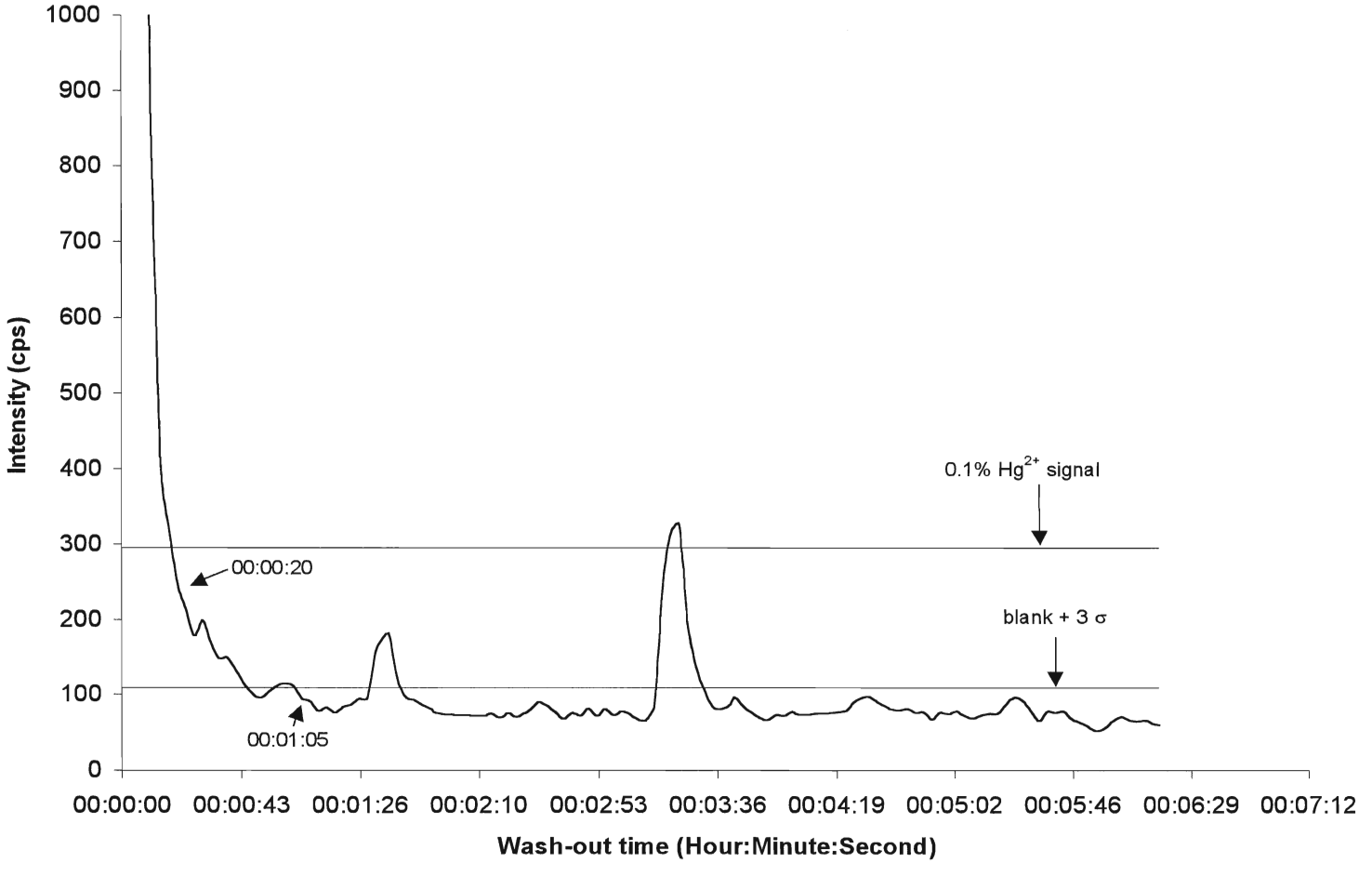


Figure 22b. 100 μg $ml^{-1}$ $Hg^{2+}$ in 1% (m/v) thiourea, 1% (v/v) HCl and 0.3% (v/v) $HNO_3$

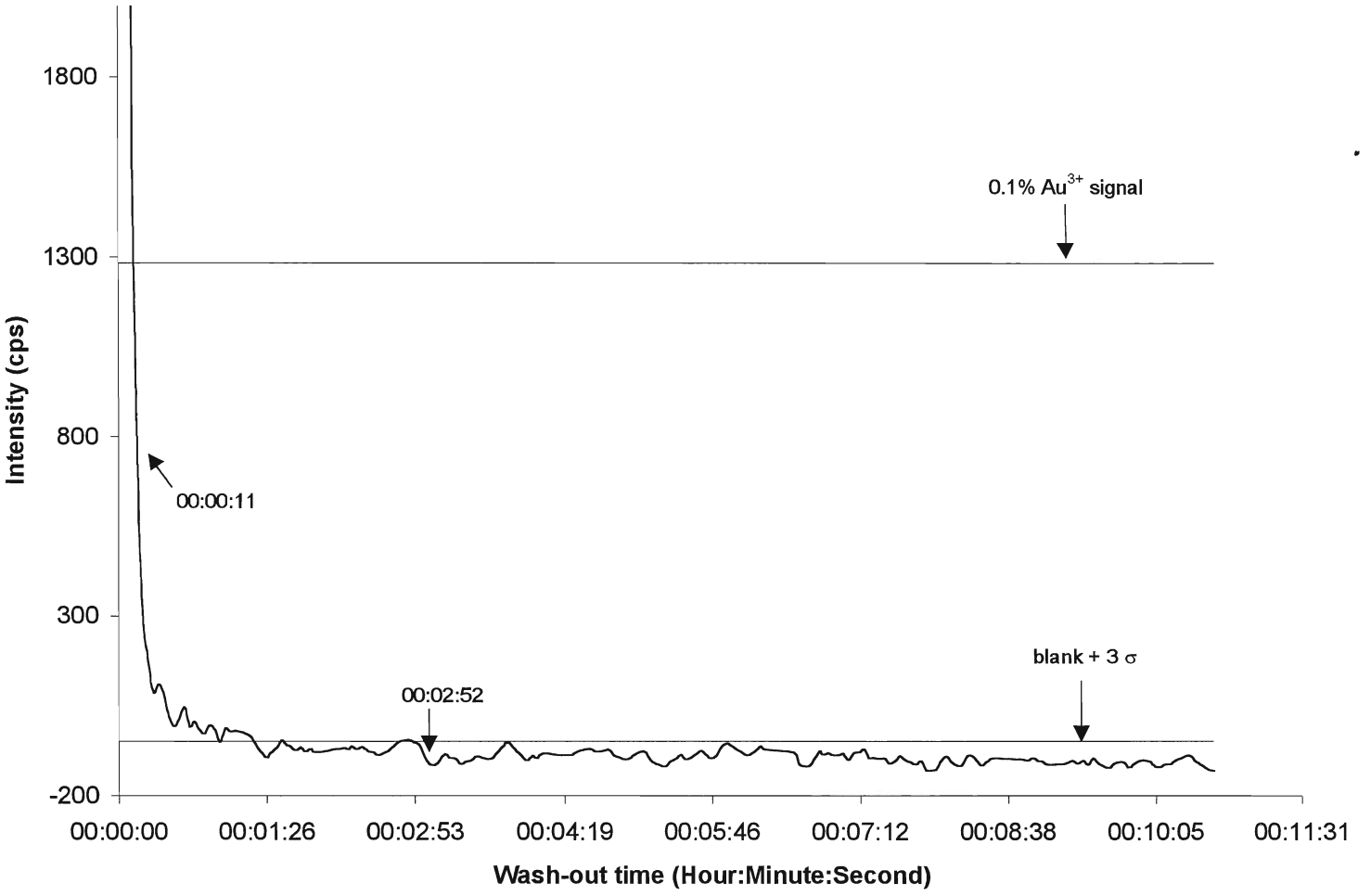


Figure 23. 100 µg ml-1 Au3+ in 2% (m/v) thiourea, 1% (v/v) HCl and 0.3% (v/v) HNO3 (with Scott-type double pass spray chamber)

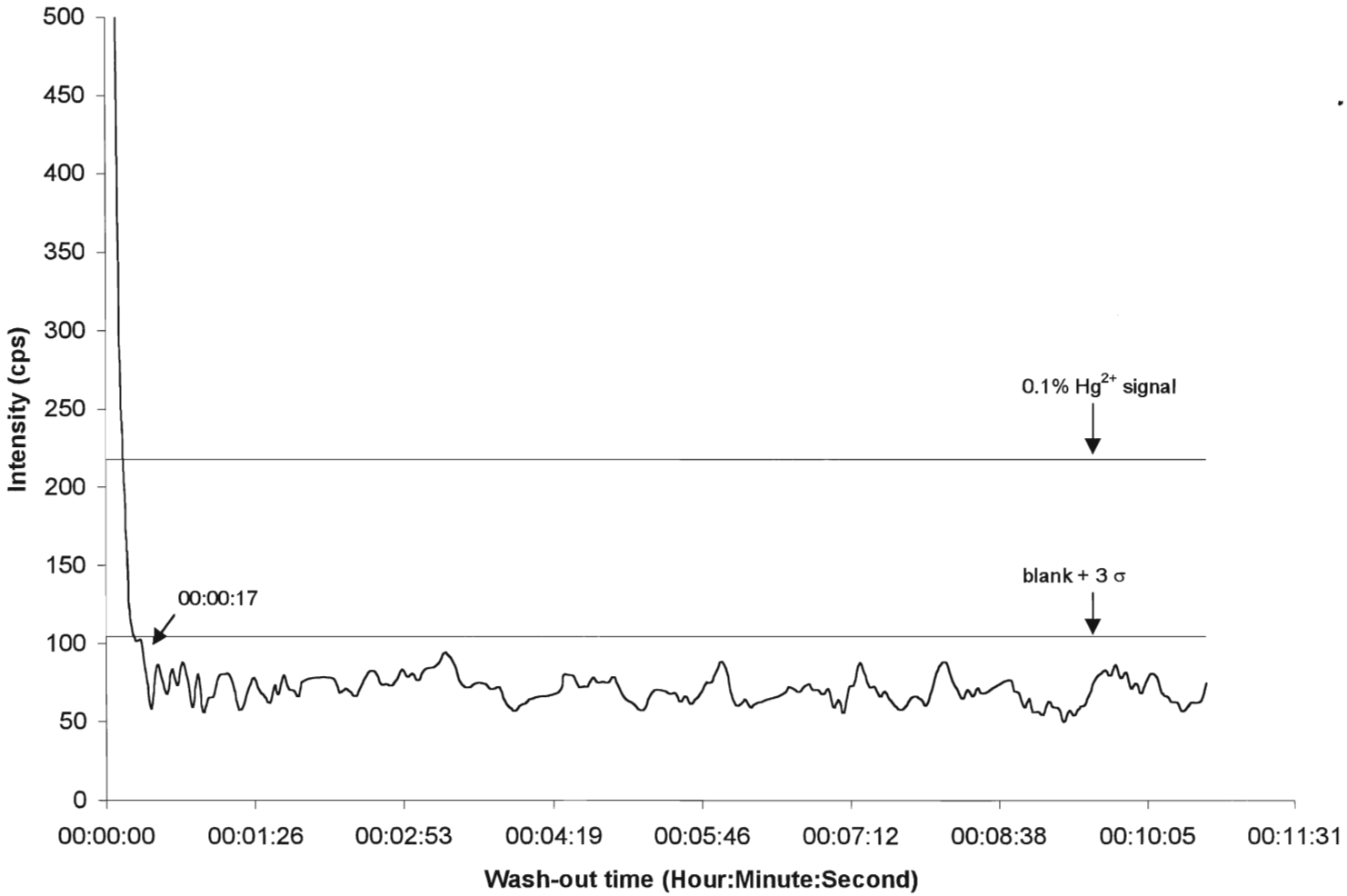


Figure 24. 100 μg $ml^{-1}$ $Hg^{2+}$ in 2% (m/v) thiourea, 1% (v/v) HCl and 0.3% (v/v) HNO3 (with Scott-type double pass spray chamber)

Some small peaks are observed on the baseline during the washing period in Figures 20b, 21b and 22b. As demonstrated in Figures 23 and 24, this effect is not observed with the use of the Scott-type spray chamber and cross-flow nebulizer combination, where a very rapid drop in the signal to less than $3\sigma$ is achieved in less than 20 seconds for $Hg^{2+}$ and 3 minutes for $Au^{3+}$. The lack of these peaks, when the double pass spray chamber is used, suggests that the occurrence is due to irregularities on the release of the sample from the surface of the cyclonic spray chamber, rather than from memory effects of the elements.

Interactions of analytes with the inner surface of the introduction system are poorly understood. Nevertheless, in order to describe the processes responsible for the memory effects of the three elements discussed, a model consistent with the experimental results can be proposed. Of the three elements of interest, gold carries the highest charge and hence is a high field strength element. Silver has the lowest charge and the shortest washout time of the three elements considered here. It is perhaps the polarizability of the ion that causes it to adsorb strongly to the surface of the tubing and the spray chamber. Reduction of the species at the walls of the introduction system is also a possibility. Gold is the most easily reducible species, followed by mercury and silver. Losses of mercury and gold from sample solutions have long plagued analysts attempting to preserve low-level concentrations of mercury and gold, suggesting that surface reduction/adsorption may be responsible for losses of the analytes. It appears that the formation of metal complexes with the reagents used in this study prevent the metals from being adsorbed, thereby inhibiting interactions of the analyte with the surface of the introduction system. This hypothesis is supported by an experiment in which a blank solution containing the

complexing agent (L-cysteine or thiourea) was introduced after a sample solution when neither reagent was present. The washout times of gold and silver did not decrease, suggesting that the sulfur-containing ligands can prevent adsorption, but cannot rapidly reverse it once it has occurred. At low concentrations of mercury and gold, L-cysteine did decrease the washout times, as defined by the 3σ criteria, to 30 seconds and 15.5 minutes respectively. The time required for a 99.9% decrease in sample signal, however, remained unchanged for both analytes.

## 4.4 Detection limits for mercury, gold, and silver

It is important to know, in addition to eliminating the memory effects from various elements, that sensitivity and detection limits are not compromised by the addition of the reagents that improve wash-in and wash-out times. It was found that signals increased for both mercury and gold in L-cysteine. In the presence of thiourea, gold signals increased as well, while mercury signals did not change. In addition, the standard deviation of the blank, for both analytes, remained the same in L-cysteine and slightly increased in thiourea. Correspondingly, detection limits, determined here as three times the standard deviation of the blank divided by calibration curve slope, for these two elements improved a little with the addition of a complexing agent. In L-cysteine, the detection limits for Au 242.795 nm and Hg 194.168 nm decreased from 2.5 to1.5 ng $ml^{-1}$ and from 12.2 to 7.5 ng $ml^{-1}$, respectively. In thiourea, the detection limits were found to be 3.8 and 12.8 ng $ml^{-1}$ for gold and mercury. The signal intensities for silver decreased, resulting in higher detection limits. In 1% (m/v) thiourea the detection limit was found to be 2.0 ng $ml^{-1}$, compared to 0.75 ng $ml^{-1}$ found in the absence of the ligand.

## 4.5 Minimization of boron memory effect

The effectiveness of mannitol as a complexing agent was tested by preparing solutions containing 1μg $ml^{-1}$ boron, 1% (v/v) nitric acid and concentrations of 1-3% (m/v) of this reagent. The results from introduction of boron in mannitol-containing solutions are shown in Figure 25. A 99.9% reduction in sample signal was obtained in times that varied from 6.5 - 12 minutes for the 1% (m/v) solution and from 6.5 - 10 minutes for the 3% (m/v) solution. Although these times represent an improvement over the washout times of 19 – 24 minutes, recorded for solutions containing only 1% (v/v) nitric acid, the washout time remains too long for routine analyses. The 3% (m/v) mannitol solution gave slightly shorter washout times, however, a small amount of crystalline material was deposited on the inner surface of the cyclonic spray chamber, suggesting that prolonged use of such high concentrations would eventually reduce the efficiency of the spray chamber.

The reaction of polyhydric alcohols with boric acid has been used for many years as a diagnostic test to identify cis diols. Hence it seemed reasonable to attempt the reaction with simpler diols. Ethylene glycol and glycerol were used at various concentrations by other students' work in our group. But they were found to be less effective than mannitol in reducing memory effect.

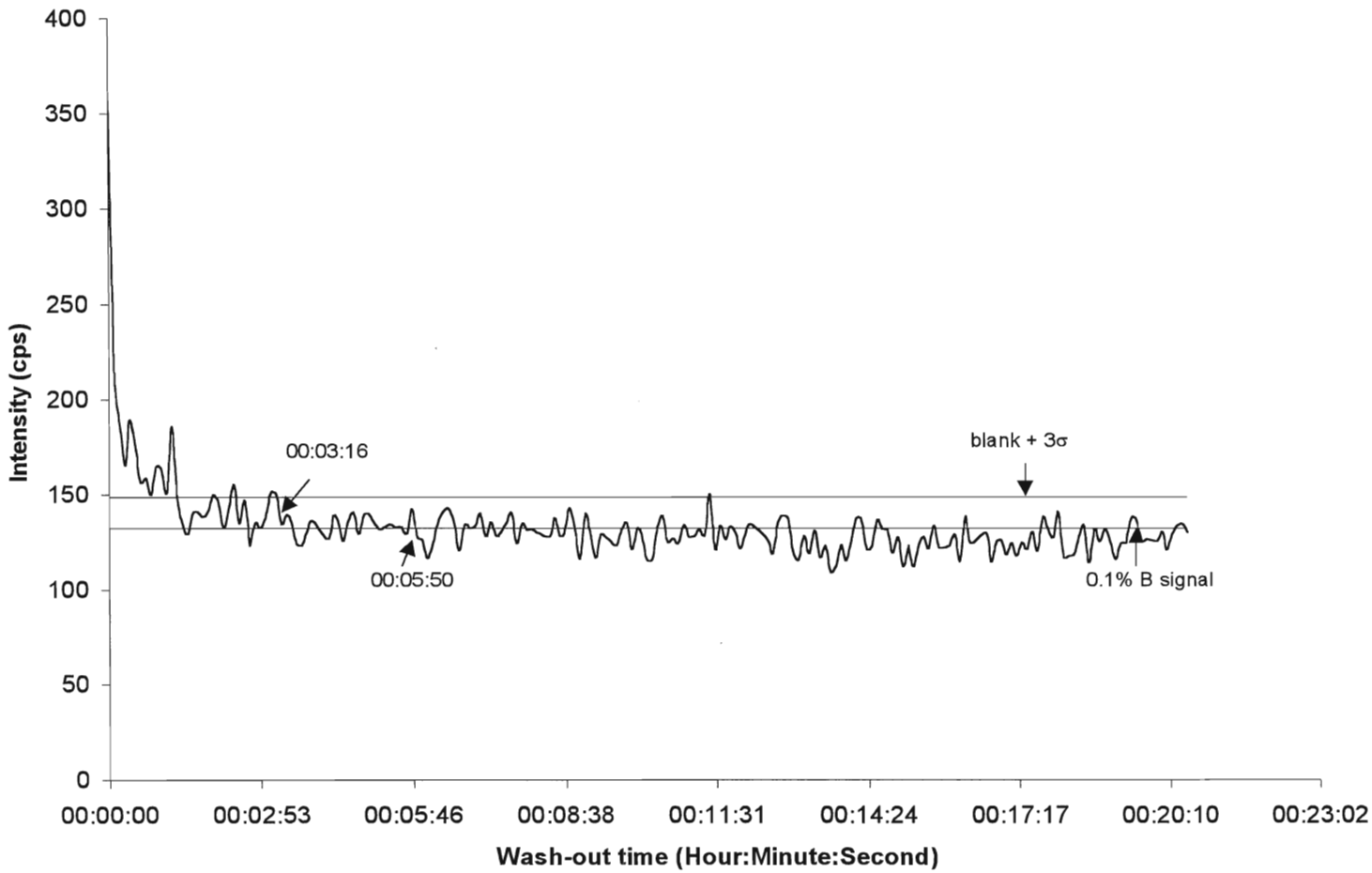


Figure 25. 1μg $ml^{-1}$ B in 3% (m/v) mannitol and 1% (v/v) $HNO_3$

# 5. Conclusions and future work

## 5.1 Conclusions and future work for pre-concentration study

Two well-ordered large surface area nanoporous materials were successfully synthesized in this work. Their ion adsorption properties were explored. They showed high loading capacity and strong selective adsorption for $Hg^{2+}$, $CH_3HgCl$, $Ag^{+}$, and $Au^{3+}$. The adsorption is independent of solution pH and the presence of $Ca^{2+}$, $Cu^{2+}$, $Cd^{2+}$, $Pb^{2+}$. The desorption can be performed by using 3% thiourea with 30% (v/v) HCl. Future work can be done on the optimization of column pre-concentration experiments. Such as the flow rate of adsorption and desorption, changing the acid type and concentration. Our work on the elimination of memory effect suggests that an eluant with thiourea and low concentration of nitric acid might work here. Another thing that should be mentioned here is that the materials are very fine powder, thus they cannot (and need not, in our experiment, we used 10mg each time) be packed in a large amount in each cartridge (or, mini-column), or else it will build up a high back-pressure while passing the water through it, just like the fine packing material for HPLC column. So it will be ideal to find out a way to spread small amount of material evenly on the surface of the filter in the cartridge.

## 5.2 Conclusions and future work for memory effect study

The memory effects of mercury, gold and silver have been completely resolved for both low and high analyte concentrations as well as in typical matrices encountered in contract laboratory analyses. The effect of the addition of L-cysteine to gold and

mercury solutions at low concentrations of around 1 $\mu g\ ml^{-1}$, and of thiourea to solutions containing silver or higher concentrations of gold and mercury improved slightly the detection limits for gold and mercury but decreases the detection limit for silver. Addition of sulfur-containing complexing agents should not decrease the accuracy of quantitative determinations of mercury, gold and silver.

This work confirms that the memory effect of boron has been reduced by the use of mannitol. However, work remains to be done to reduce the wash-out time to the point where boron determinations can be carried out at the same rate as other elements.

# References:


[1] A. Montaser, D.W. Golightly, *Inductively Coupled Plasma in Analytical Atomic Spectrometry,* VCH publishers, Inc. New York, 1992.

[2] J. W. Robinson, *Undergraduate Instrumental Analysis,* Marcel Deckker Inc., New York, 1995, 5th. Ed., p443-494.

[3] P. C. Rudner, J.M.C. Pavon, A.G. de Torres, F.S. Rojas, *Fresenius' J. Anal. Chem.,* 1995, **352**, 615.

[4] J. P. Ghosh, H.R. Das, *Talanta,* 1981, **28**, 274.

[5] C. Sazarnini, V. Porta, E. Mentasti, *New J. Chem.,* 1989, **13**, 463.

[6] U. Pyell, G. Stork, *Fresenius' J. Anal. Chem.,* 1992, **342**, 281.

[7] M. Volkan, O. Y. Ataman, A. G. Howard, *Analyst,* 1987, **112**, 1409.

[8] P. Y. T. Chow, F. F. Cantwell, *Anal. Chem.,* 1988, **60**, 1569.

[9] T. Seshardi, G. Dietz, H. I. Haupt, *Fresenius' Z. Anal. Chem.,* 1984, **319**, 403.

[10] M. E. Mahmoud, *Anal. Lett.,* 1996, **26**, 1791.

[11] K. Ohshima, H. Watanabe, K. Haraguchi, *Anal. Sci.,* 1986, **2**, 131.

[12] P. Burba, P.G. Willmer, R. Klockenkaemper, *Vom Wasser* 1988, **71**, 179 (CA: 110:141092).

[13] W. Guo, X. Zeng, H. Li, Y. Jian, *Huaxue Fence*,1994,30, 289.

[14] G.M. Varshal, T.K. Velyukhanova, V.I. Pavlutskaya, N.P. Starshinova, A.A. Formanovsky, I.F. Seregina, A.M. Shilnikov, G.I. Tsysin, Y.A. Zolotov, *Int. J. Environ. Anal. Chem.,* 1994, **57**, 107.

[15] N. P. Starshinova, E. M. Sedykh, G. I. Tsyzin, I. A. Kovaley, *Proc. - Semin. At. Spectrochem.,* 14th (1998), 292-295. Editor(s): Krakovska, Erika; Ruzickova, Silvia. Publisher: Stroffek (CA: 130:118777).

[16] G.V. Myasoedova, Nataliya I. Shcherbinina, Oksana N. Grebneva, *Anal. Sci.* (1995), 11, 181.

[17] M. Lopez-Artiguez, A. Camean, M. Repetto, *At. Spectrosc.* 1996, 17, 83.

[18] Y. Lin, Z. Gong, Z. Zhuang, Z. Deng, X. Wang, *Fenxi Kexue Xuebao,* 1995, 11, 16.

[19] M.E. McComb, H.D. Gesser, *Talanta,* 1999, **49**, 869.

[20] K. Brajter, E. Dabek-Zlotorzynska, *Talanta,* 1986, **33**, 149.

[21] H. Nishide, J. Deguchi, E. Tsuchida, *Chem. Lett.,* 1976, **2**, 169.

[22] C.T. Kresge, M.E. Leonowicz, W.J. Roth, J.C. Vartuli, J.S. Beck, *Nature,* 1992, **359**, 710.

[23] J.S. Beck, J.C. Vartuli, W.J. Roth, M.E. Leonowicz, C.T. Kresge, S.B. McCullen, J.B. Higgins, J.L. Schlenker, *J. Am. Chem. Soc.* 1992, **114**, 10834.

[24] S.B. McCullen, J.C. Vartuli, C.T. Kresga, W.J. Roth, J.S. Beck, K.D. Schmitt, M.E. Leonowicz, J.L. Schlenker, S.S. Shih, J.D. Lutner, *Access in Nanoporous Materials,* T.J. Pinnavaia, M.F. Thorpe (editors). Plenum Press, New York, 1995, p8.

[25] Peter T. Tanev, T.J. Pinnavaia, *Access in Nanoporous Materials,* T.J. Pinnavaia, M.F. Thorpe (editors). Plenum Press, New York, 1995, p18-20.

[26] G. Engelhardt, D. Michel, *High Resolution Solid-State NMR of Silicates and Zeolites,* John Wiley and Sons, Toronto, 1987.

[27] M. Pursch, A. Schneller, T. Schneller, R. Brindle, K. Albert, E. Linder, *Chem. Mat.,* 1996, **8**, 1245.

[28] R.F. Browner, A.W. Boorn, *Anal. Chem.,* 1984, **56,** 787A.

[29] C.E. McGinnis, J.C. Jain, and C.R. Neal, *Geostandards Newsletter,* 1997, **21**, 289.

[30] A. Stroh, E. Denoyer, Q. Lu and U.Völlkopf, *Optimization and Use of Flow Injection Vapor Generation,* Perkin-Elmer Corporation, Norwalk, CT, 1993.

[31] A. Newman, *Anal.Chem.,* 1986, **68**, 46A.

[32] A.Al-Ammar, R.K. Gupta and R.M. Barnes, *Spectrochim. Acta,* 1999, **54B**, 1077 and references cited.

[33] E. Fatemian, J. Allibone and P.J. Walker, *Analyst,* 1999, **124**, 1233.

[34] A.W. Varnes, *J. Anal. At. Spectrom.,* 1988, **3**, 803.

[35] L.S. Dale and S.J. Buchanan, *J. Anal. At. Spectrom.*, 1986, **1**, 59.

[36] J.A. Moreton and H.T. Delves, *J. Anal. At. Spectrom.,* 1998, **13**, 659.

[37] M. Totland, Atomic Energy Canada Ltd., Deep River, Ontario, Canada, Personal Communication.

[38] E. Beary, National Institute for Standards and Technology, Gaithersburg, Maryland, USA, Personal Communication.

[39] L. Mercier, Thomas J. Pinnavaia, *Advanced Materials,* 1997, **9**, 500.

[40] P.T. Tanev, T.J. Pinnavaia, *Science,* 1995, **267**, 865.

[41] M.H. Lim, C.F. Blandford, Andreas Stein, *Chem. Mater.,* 1998, **10**, 467.

[42] M.S. Iamamoto, Y. Gushikem, *J. Colloid Interface Sci.*, 1989, **129**, 162.

[43] E.I.S. Andreotti, Y. Gushikem, *J. Colloid Interface Sci.,* 1991, **142**, 97.

[44] W.C. Moreira, Y. Gushikem, O.R. Nascimento, *J. Colloid Interface Sci.,* 1992, **150**, 115.

[45] J. C. Miller, J. N. Miller, *Statistics for Analytical Chemistry,* Ellis Horwood Limited, 1993, Totonto, 3rd Ed. p118.

[46] I. D. Brindle, unpublished results.

[47] G.E. Rodgers, *Introduction to coordination, solid state, and descriptive inorganic chemistry,* McGraw-Hill, Inc., 1994, Toronto. p128.

[48] F. A. Cotton, G. Wilkinson, *Advanced Inorganic Chemistry,* John Wiley & Sons, Toronto. 5th. Ed., p 597-598.

[49] D.R. Lide (Editor-in-chief), *Handbook of chemistry and physics,* CRC press, New York, 76th Ed. 1995.